Precambrian Research 249 (2014) 144–161

Contents lists available at ScienceDirect

Precambrian Research

journal homepage: www.elsevier.com/locate/precamres

# Early Neoproterozoic accretionary assemblage in the Cathaysia Block: Geochronological, Lu–Hf isotopic and geochemical evidence from granitoid gneisses

Yuejun Wang[a,b,c,*], Yuzhi Zhang[a,*], Weiming Fan[d], Hongyan Geng[e], Heping Zou[a,b], Xianwu Bi[c]

[a] Department of Earth Sciences, Sun Yat-Sen University, Guangzhou 510275, China
[b] Guangdong Provincial Key Laboratory of Mineral Resources and Geological Processes, Guangzhou 510275, China
[c] State Key Laboratory of Ore Deposit Geochemistry, Institute of Geochemistry, Chinese Academy of Sciences, Guiyang 550002, China
[d] Key Laboratory of Continental Collision and Plateau Uplift, Institute of Tibetan Plateau Research, Chinese Academy of Sciences, Beijing 100101, China
[e] Department of Earth Sciences, The University of Hong Kong, Pokfulam Road, Hong Kong, China

ARTICLE INFO

*Article history:*
Received 24 January 2014
Received in revised form 5 May 2014
Accepted 10 May 2014
Available online 21 May 2014

*Keywords:*
Zircon U–Pb geochronology
Lu–Hf isotopic composition
Geochemistry
Early neoproterozoic granitic gneiss
Accretionary assemblage
Cathaysia

ABSTRACT

The South China Block (SCB) is composed of the Yangtze Block in the northwest and the Cathysia Block in the southeast. The earliest Neoproterozoic granitic rocks in the SCB are important for our understanding of the tectonic regime and location of this ancient continent in relation to the Rodinia supercontinent. However, such rocks have rarely been reported for the Cathaysia Block so far. In this study, six granitic gneisses from the Wuyi-Yunkai domain gave zircon U–Pb ages of 985–913 Ma, indicating the presence of the early Neoproterozoic granitic magmatism in the Cathaysia interior. These granitic gneisses are peraluminous with high FeOt, MgO, $TiO_2$ and CaO/$Na_2O$ but low $SiO_2$, $Al_2O_3/TiO_2$, $Al_2O_3/(MgO + FeOt)$ and Rb/Sr ratios. They show steep REE chondrite-normalized patterns with δEu values of 0.35–0.70. These samples have strongly negative Ba, Sr, Nb-Ta, P and Ti anomalies in primitive mantle-normalized diagrams, and $\varepsilon Nd(t)$ values of −9.54 to −3.81, similar to those of the Kwangsian granitic rocks and Precambrian volcanosedimentary package in the Cathysia Block. The zircon grains with the earliest Neoproterozoic age gave $\varepsilon Hf(t)$ values of −9.64 to +2.78 with the peak values at −2.5 and −7.5, and Hf model ages of 1.35–2.00 Ga with the two-peaks of 1.57 Ga and 1.75 Ga, respectively. These data suggest that the granitic gneisses originated dominantly from a binary mixing of metapelitic and metaigneous components, with insignificant input of juvenile materials. We consider that these rocks are closely related to the closure of the earliest Neoproterozoic (~980 Ma) Wuyi-Yunkai back-arc basin in an accretionary continental margin setting. In combination with other data, it is proposed that the previously-defined Cathaysia block might consist of various sub-blocks separated by the arc-back-arc basin prior to the early Neoproterozoic period. The Wuyi-Yunkai arc-back-arc system was finally closed at ~920 Ma, significantly younger than the classical Grenvillian Orogenic event, and thus the SCB was located on the margin of the Rodinia supercontinent.



## 1. Introduction

The amalgamation process of the Yangtze and Cathaysia Blocks to form the South China Block (SCB) and the location of the united SCB in the Rodinia supercontinent has been a hotly debated issue. Two major viewpoints have been proposed. One believed that the SCB finally amalgamated at the end of the Mesoproterozoic along the Jiangnan orogen (inset in Fig. 1) and occupied an intra-cratonic position of the Rodinia (e.g., Li et al., 1995, 2008b,c, 2002, 2009; Ye et al., 2007). However, recent studies indicated that the formation of the Jiangnan orogen probably occurred at ~820–830 Ma, significantly later than the assembly time of the Rodinia (e.g., Zhou et al., 2009; Wang et al., 2006; Wang et al., 2007a,b; Wang et al., 2008a, 2011b; Wu et al., 2006; Zhao et al., 2011; Zhang et al., 2011a, 2012a,b, 2013). The other group of researchers suggested that the SCB was either located on the margin of Rodinia or external to the supercontinent (e.g., Torsvik et al., 2001; Yang et al., 2004; Wang et al., 2013a,b; Cawood et al., 2013 and reference therein). The

* Corresponding authors at: Department of Earth Sciences, Sun Yat-Sen University, No. 135, Xingang Xi Road, Guangzhou 510275, People's Republic of China. Tel.: +86 20 84111209; fax: +86 20 84111209.
*E-mail address:* wangyuejun@mail.sysu.edu.cn (Y. Wang).

http://dx.doi.org/10.1016/j.precamres.2014.05.003
0301-9268/

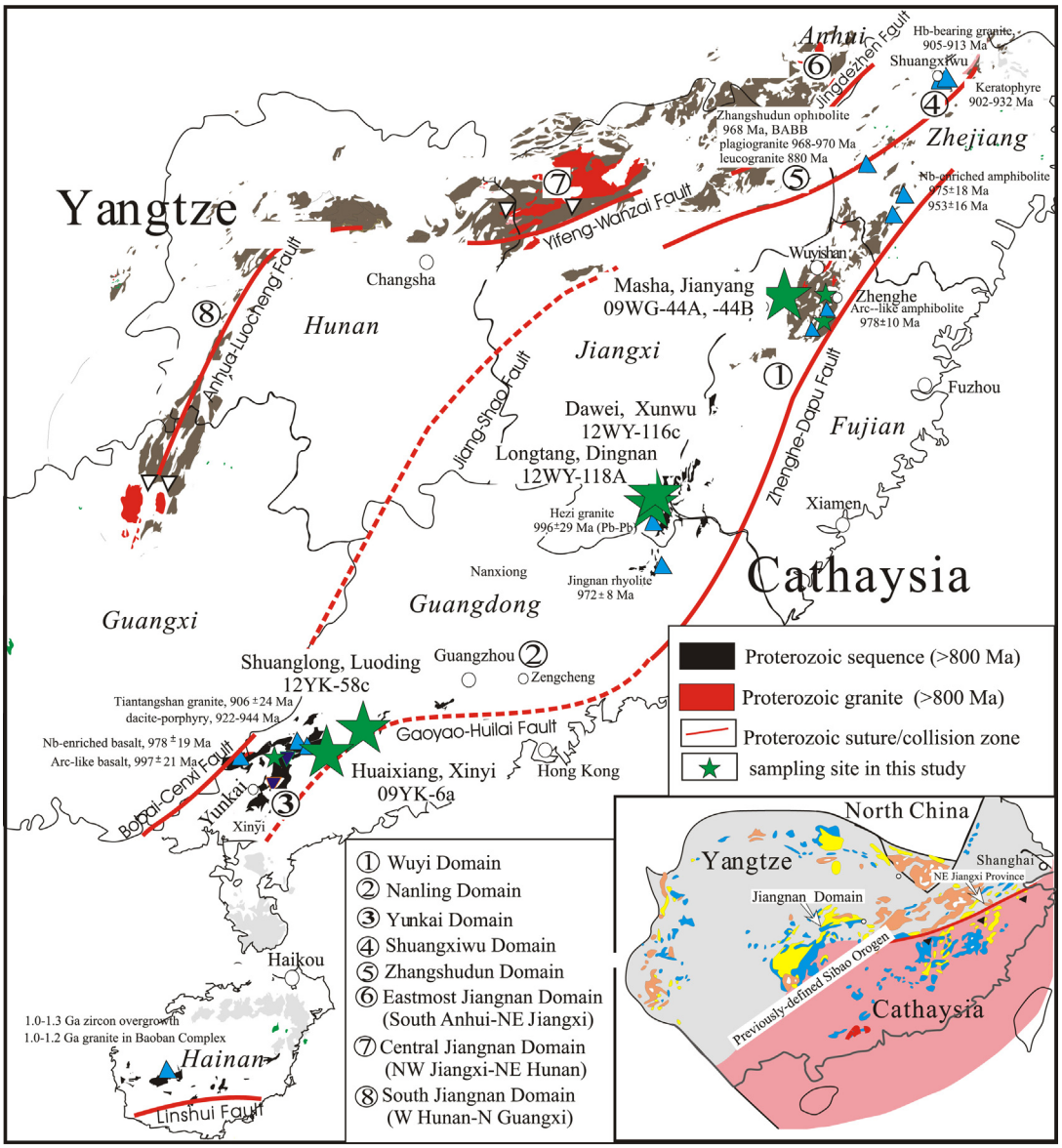


**Fig. 1.** A simplified geological map showing the location of the early Neoproterozoic granitic plutons in the eastern South China Block (revised from Wang et al., 2013a,b). Also shown are the reported early Neoproterozoic igneous rocks in the Cathaysia. Inset shows the previously-defined Sibaoian (~1.0 Ga) orogenic belt by the assemblage of the Yangtze and Cathaysia Blocks (after Zhang et al., 2012b).

main reason behind the debate is the lack of data and insufficient knowledge on the earliest Neoproterozoic geological history of the Cathaysia Block when the Rodinia was assembled.

Numerous studies have been carried out on the Neoproterozoic tectonic evolution of the Jiangnan orogen (e.g., Zhao and Cawood, 1999, 2012; Zhou et al., 2009; Wang et al., 2006, Wang et al., 2007a,b; Wang et al., 2008a, 2011a; Zhang et al., 2013 and references therein). However, the expected earliest Neoproterozoic (~0.95 Ga) rock associations were absent in the South Anhui, NW Jiangxi, NE and SW Hunan and NE Guangxi areas of the Jiangnan orogen (Fig. 1; e.g., Li and Li, 2003; Wu et al., 2006; Ye et al., 2007; Li et al., 2008a,b,c, 2009; Gao et al., 2009). This made many researchers question whether a tectonic event really took place in the earliest Neoproterozoic in the SCB. On the other hand, zircons inherited from the Cathaysia basement of the SCB and detrital grains from the metamorphic sedimentary rocks gave abundant U–Pb ages of ~0.90–1.00 Ga, distinct from those from the Jiangnan orogen (e.g., Yu et al., 2007; Wang et al., 2007c, 2010a,b; Wan et al., 2007, 2010; Li et al., 2011; Zhao et al., 2011; Zhou et al., 2009; Wang et al., 2012c, 2013a,b). In addition, Wang et al. (2013a,b) and Zhang et al. (2013) recently identified the ~985–970 Ma metabasites from the Wuyi-Yunkai area of the Cathaysia Block with a geochemical affinity to arc and back-arc basin volcanic rocks.

In this study, we document zircon U–Pb geochronological and Lu–Hf isotopic data and whole-rock elemental and Sr–Nd isotopic results for granitic gneiss and migmatite (described herein as granitic gneisses) from the Wuyi-Yunkai domain of the Cathaysia Block. Our data revealed the presence of 985–913 Ma granitic rocks, which were partial melting products of the metavolcanic-sedimentary rocks. These data place critical constraints on the tectonic history of the SCB in the earliest Neoproterozoic and define its location on the margin of the Rodinia.

## 2. Geological setting and petrography

The Yangtze basement is composed of an Archean-Paleoproterozoic crystalline nucleus (e.g., TTG rocks, felsic gneisses and amphibolites) in the northern Hubei Province and widespread

Neoproterozoic igneous and sedimentary rocks (e.g., Gao et al., 1999, 2011; Qiu et al., 2000; Zheng et al., 2007, 2008; Jiao et al., 2009). However, in the Cathaysia Block, the Neoarchean basement is poorly found and the Paleoproterozoic migmatite, granitoid gneisses and amphibolite only outcropped in NW Zhejiang and NE Fujian Provinces (e.g., Fujian BGMR, 1985; Zhejiang BGMR, 1989; Liu et al., 2008; Yu et al., 2009, 2010; Shu et al., 2008). The amalgamation of the Yangtze and Cathaysia Blocks finally formed the united SCB along the Jiangnan Orogen or Jiangshan–Shaoxing suture in the early Neoproterozoic period (e.g., Charvet et al., 1996; Wang et al., 2006; Wang et al., 2007a,b; Zhang et al., 2012a, 2013 and references therein). The coherent SCB is unconformably overlain in turn by an upper Neoproterozoic-lower Paleozoic, Devonian- lower Triassic and upper Triassic-lower Jurassic packages (e.g., Wang and Li, 2003; Shu et al., 2008, 2011; Yu et al., 2010; Wan et al., 2010; Wang et al., 2010a,b, 2013a,b).

The Cathaysia Block can be subdivided into the eastern and western Cathaysia separated by the Zhenghe-Dapu fault, which are extensively outcropped by Mesozoic volcanic rocks of SE Coastal Provinces and Precambrian metamorphic rocks of the Wuyi, Nanling and Yunkai domains, respectively (e.g., Fujian BGMR, 1985; Xu et al., 2005; Wang et al., 2012c, 2013a,b). In these metamorphic domains of the western Cathaysia, the main metamorphic rocks are exposed sparsely as tectonic inliers and contain the greenschist- to amphibolite-facies paragneiss, mica schist, paragneiss, quartzite, marble, granitoid gneiss, migmatite and amphibolite with a small amount of metavolcanic rocks. They are intruded by early Paleozoic to late Mesozoic granites and covered by Mesozoic volcanic and sedimentary rocks. According to the lithological and metamorphic features, the metamorphic rocks were previously mapped as the lower and upper sequence of the Cathaysia basement. The lower sequence consists of biotite-plagioclase leptynite, sillimanite-mica schist, migmatite, gneiss and amphibolite, which is traditionally termed as the Mayuan Group in NW Fujian, Chencai and Badu Group in SW Zhejiang, Hezi/Xunwu Group in SE Jiangxi and Yunkai Group in SW Guangdong. The upper sequence is defined as the Mamianshan Group in Fujian, Longquan Group in Zhejiang and Taoxi Group in NE Guangdong (Fig. 1; e.g., Fujian BGMR, 1985; Zhejiang BGMR, 1989). The high-grade metamorphic rocks predominantly developed in the lower sequences including the previously-defined Badu, Chencai, Mayuan, Hezi/Xunwu and Yunkai Groups along the Wuyi, Nanling and Yunkai domains (e.g., Fujian BGMR, 1985; Zhejiang BGMR, 1989; Guangdong BGMR, 1988). However, new geochronological data show that, in the previously-defined Cathaysia basement, part of the migmatite, granitoid gneisses and amphibolite in northwestern Zhejiang and northern Fujian Provinces formed in the Paleoproterozoic era (e.g., Fujian BGMR, 1985; Zhejiang BGMR, 1989; Liu et al., 2008; Yu et al., 2009, 2010; Shu et al., 2008). In contrast, a large amount of the schist, granitoid gneiss, migmatite and volcanoclastics rocks were recently dated at the Neoproterozoic and even early Paleozoic period (e.g., Wan et al., 2007, 2010; Li et al., 2010; Zeng et al., 2008; Charvet et al., 2010; Yu et al., 2009, 2010a,b; Wang et al., 2007a,b, 2011a,b 2012c, 2013a,b and references therein). In addition, a small amount of amphibolite, metagabbro and metadiabase occur as lens, pods and fragments, which might be the relicts of the earliest Neoproterozoic arc-back-arc system in the Cathaysia block (e.g., Wang et al., 2013a,b; Zhang et al., 2012a).

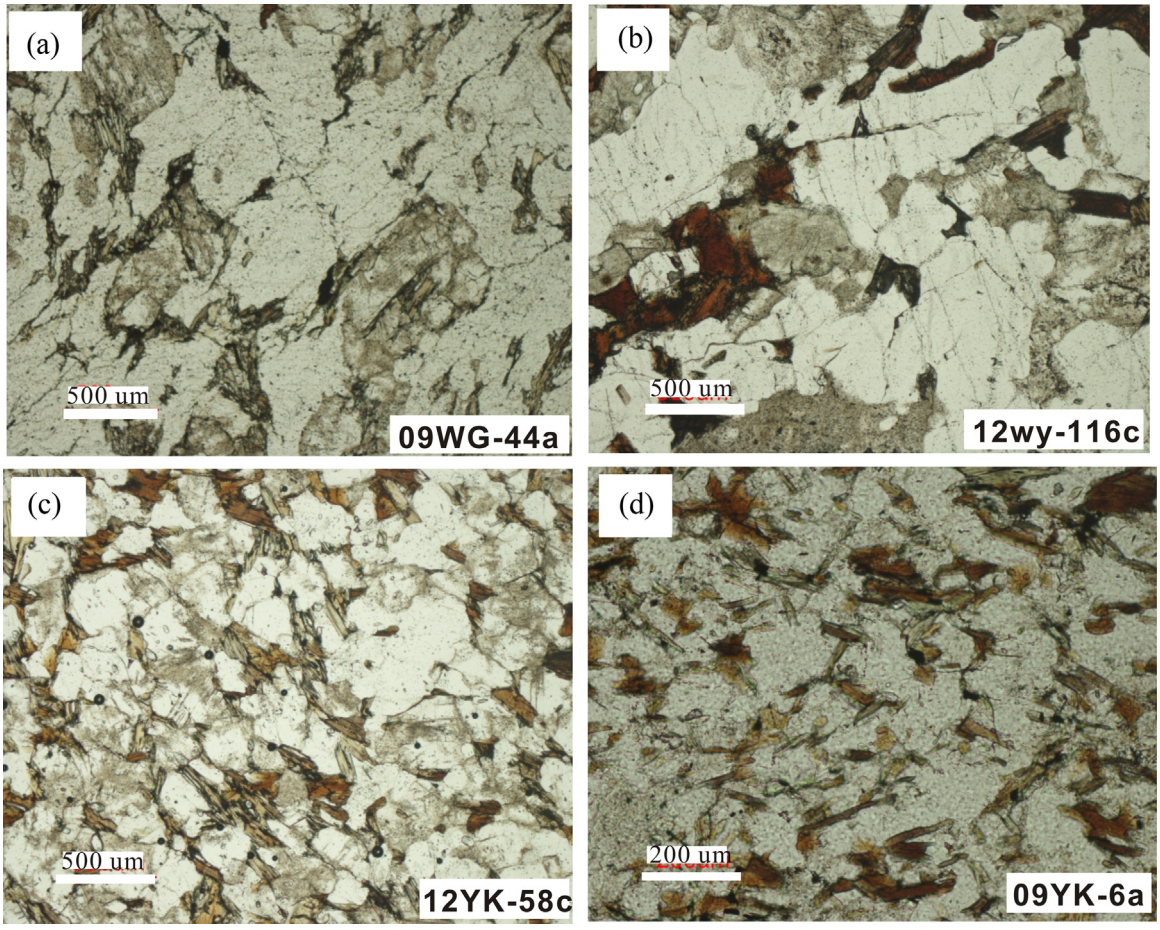


**Fig. 2.** Microscope photographs for representative granitic rocks: (a) 09WG-44a, (b) 12wy-116c, (c) 12YK-58c and (d) 09YK-6a.

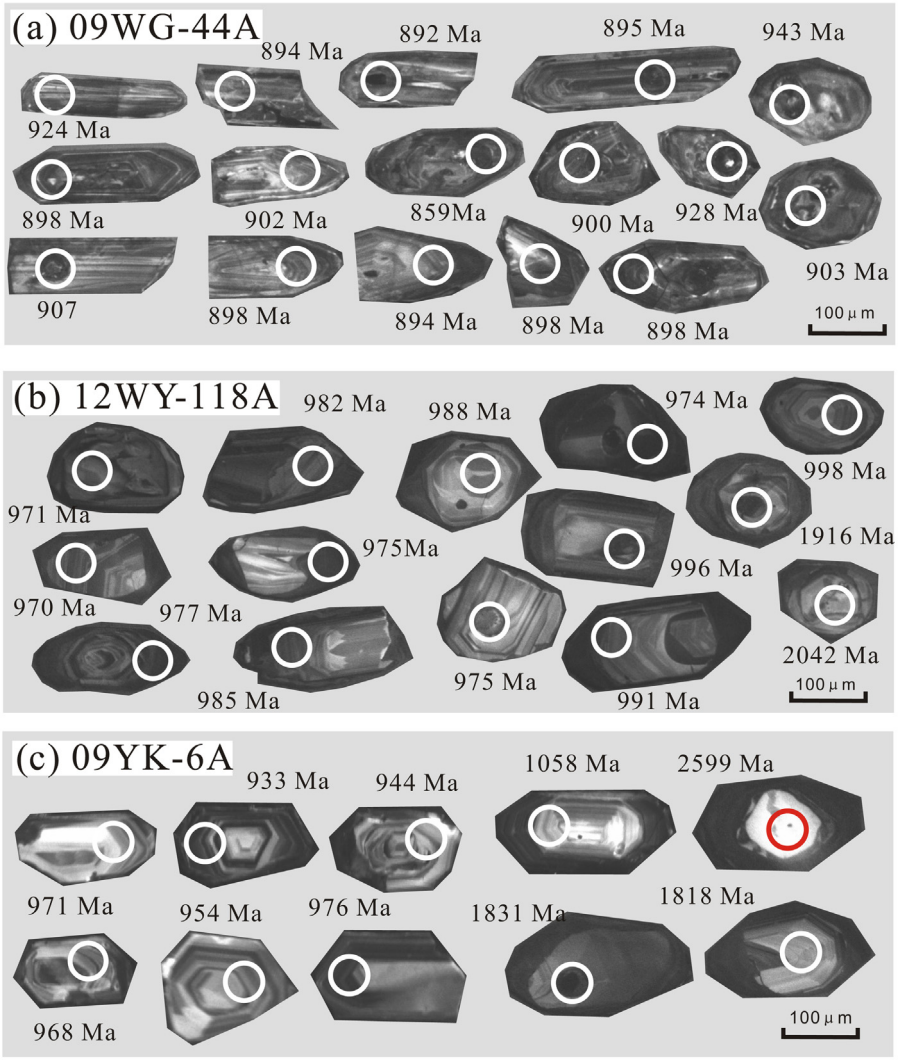


**Fig. 3.** CL images of representative zircons for granitic samples (a) 09WG-44A, (b) 12WY-118A and (c) 09YK-6A.

In this paper, we focus on the granitoid gneisses in the lower sequence of the Cathaysia basement, which were collected from Masha and Shibei (North Wuyi), Dawei (Xunwu in Nanling), Longtang (Dingnan), Shuanglong(Luoding) and Huaixiang (Xinyi) (Fig. 1). They appear either as leucosomes of migmatites and gneisses (e.g., Masha and Xinyi areas) with strong magmatic orientation or gneissic and mylonitic granite with post-magmatic ductile deformation (e.g., Longtang and Hezi areas). Their crystallization ages is poorly constrained so far. The principal mineral phases of the granitoid gneisses are plagioclase (~25–38%), K-feldspar (~26–34%), quartz (~15–35%) and biotite (~10–20%), with minor amounts of accessory minerals of apatite, zircon, monazite and Fe–Ti oxides (Fig. 2a–d). Among these rocks, several samples additionally contain muscovite (3–5%). The samples from the Nanling area commonly show a porphyritic texture with feldspar phenocrysts in a groundmass of fine-grained K-feldspar, plagioclase and quartz.

## 3. Analytical methods

Zircon grains for U–Pb dating and Lu–Hf isotopic compositions were separated using conventional heavy liquid and magnetic techniques. Their internal structure was examined by cathodoluminescence image at the Guangzhou Institute of Geochemistry (GIG), the Chinese Academy of Sciences (CAS). U, Th and Pb isotopic measurements for 09WG-44B were undertaken using the Cameca IMS 1280 large-radius SIMS at the Institute of Geology and Geophysics (CAS) and other samples by Nu instruments MC-ICP-MS attached to the M-50-HR Excimer Laser Ablation System at the University of Hong Kong. The instrumental setting and detailed analytical procedures for two techniques were described in Li et al. (2009) and Xia et al. (2004), respectively. Common Pb correction was made using the observed $^{204}$Pb peak. Data processing was carried out via the SQUID 1.03 and Isoplot/Ex 2.49 programs of Ludwig (2001). Zircon in situ Lu–Hf isotopic compositions were measured by Nu instruments MC-ICP-MS at the University of Hong Kong. External calibration was made by measuring zircon standard 91,500 with the unknowns during the analyses to evaluate the reliability of the analytical data, which yielded a weighted mean $^{176}$Hf/$^{177}$Hf ratio of 0.282307 ± 31 (2σ, Wu et al., 2006).

The representative samples were crushed to 200-mesh in a steel mortar and ground in a steel mill for the elemental and isotopic analyses. The whole-rock major oxides and trace element contents, along with Sr–Nd isotopic ratios for the samples were performed on X-ray fluorescence spectrometry, Elan6000 inductively coupled plasma mass spectrometer and MC-ICPMS at the GIG, CAS, respectively. The detailed sample preparation and chemical separation procedures were described by Wei et al. (2002) and

Liang et al. (2003). The mass fractionation corrections for isotopic ratios are based on $^{86}Sr/^{88}Sr = 0.1194$ and $^{146}Nd/^{144}Nd = 0.7219$. The measured $^{87}Sr/^{86}Sr$ ratios of the SRM 987 standard and $^{143}Nd/^{144}Nd$ ratios of the La Jolla standard are $0.710265 \pm 12$ ($2\sigma$) and $0.511862 \pm 10$ ($2\sigma$), respectively. Within-run errors of precision for these analyses are estimated to be better than 0.000015 for $^{146}Nd/^{144}Nd$ in the 95% confidence level. $^{87}Rb/^{86}Sr$ and $^{147}Sm/^{144}Nd$ ratios were calculated using the Rb, Sr, Sm and Nd contents measured by ICP-MS.

## 4. Zircon U–Pb and Lu–Hf isotopic results

Six samples (see Fig. 1 for the sampling locations) were selected for zircon U–Pb dating and in situ Lu–Hf isotopic measurement. The separated zircons from these samples are mostly transparent and euhedral in morphology. The internal texture is featured by oscillatory zonation in CL images, similar to those of acid igneous grains (Fig. 3a–c). The zircon U–Pb and in situ Lu–Hf isotopic analytical data are listed in Tables 1 and 2. The sampling location and dating results are summarized in Table 3.

09WG-44A and 09WY-44B samples from Masha (Jianyang) were selected for LA-ICPMS and SIMS zircon U–Pb dating, respectively. Twenty-five analyses for 09WG-44A form a discordia line with the upper intercept age of $907 \pm 28$ Ma and twenty concordant spots yield a weighted mean age of $909 \pm 10$ Ma (MSWD = 0.5, Fig. 4a). Their $\varepsilon Hf(t)$ values range from −5.2 to +0.5 and Hf two-stage model ages from 1.43 Ga to 1.65 Ga, respectively (Table 1). Twenty-four spots on 09WY-44B grains, which show the typical CL image of igneous grains (Fig. 2a), have variable Th/U ratios of 0.10–1.10. These analytical spots constitute a discordia line with the upper intercept age of $906 \pm 18$ Ma. Eighteen spots of them give a weighted mean age of $916 \pm 6$ Ma (MSWD = 1.0, Fig. 4b), with $\varepsilon Hf(t)$ of −5.7∼ +2.8 and $T_{DM}$ of 1.35–1.69 Ga (Tables 2 and 3). The 38 concordant spots for the two samples together give a $^{206}Pb/^{238}U$ weighted mean age of $913 \pm 5$ Ma (MSWD = 0.5) with the $\varepsilon Hf(t)$ values peaking at −2.3. This age can be interpreted as the crystallization age of the Masha granitic gneiss.

Two gneissoid samples (12WY-116C and -118A) were taken from Dawei (Xunwu) and Longtang (Dingnan), respectively (Fig. 1). Fourteen grains from 12WY-116C have $^{207}Pb/^{206}Pb$ apparent ages ranging from 1092 Ma to 2653 Ma, with variable $\varepsilon Hf(t)$ values (−9.5 to 12.5) and Neoarchean-Proterozoic model ages (2.56 Ga to 2.82 Ga). Four spots (12WY- 116C-01, -25, -29 and -30) show the apparent age of $^{207}Pb/^{206}Pb > {}^{207}Pb/^{235}U > {}^{206}Pb/^{238}U$, suggestive of Pb loss during later tectonothermal events. The remaining eight analyses have Th/U ratios = 0.14–1.60 and give a weighted mean age of $982 \pm 27$ Ma (MSWD = 0.5, Fig. 5a). The earliest Proterozoic grains show variable $\varepsilon Hf(t)$ values with two clusters at −8.5 and −2.5, respectively, and $T_{DM}$ model ages from 1.48 Ga to 1.89 Ga (Table 3). For 12WY-118A, one cluster defined by 18 out of 27 grains yields a weighted mean age of $963 \pm 11$ Ma (Fig. 5b). Their Th/U ratios are 0.29–1.59 and $\varepsilon Hf(t)$ values vary from −7.7 to −0.4 with two peaks of −6.8 and −1.9. Their $T_{DM}$ model ages range from 1.49 Ga to 2.00 Ga (Table 3). Four analyses from 12WY-118A have older $^{207}Pb/^{206}Pb$ apparent ages of 1265–2786 Ma, interpreted as inherited grains.

12YK-58C and 09YK-6A, the gneissic enclave and granitoid gneiss from Shuanglong (Luoding) and Huaixiang (Xinyi), respectively, were previously mapped as the Yunkai Group (Fig. 1). Seven grains from 12YK-58C give the older U–Pb apparent age (1475–1995 Ma) and yield upper intercept age of $2028 \pm 48$ Ma. The remaining 19 spots for 12YK-58C have Th/U ratios of 0.26–1.34 and constitute a well-defined discordant line with upper intercept age of $926 \pm 28$ Ma (Fig. 6a). These grains give $\varepsilon Hf(t)$ values of −7.3 to −5.5 with peak at −6.8 and $T_{DM}$ of 1.68–1.76 Ga (Tables 2 and 3).

**Table 1**
Results of SIMS zircon U–Pb analyses for the 09WY-44B granitoid gneiss in the Wuyi Domain, Cathaysia Block.

| spot | Th/U | Isotopic ratios | | | | Apparent age (Ma) | | | | Dis | $^{176}Hf/^{177}Hf$ | 2σ | $^{176}Lu/^{177}Hf$ | $^{176}Yb/^{177}Hf$ | $\varepsilon Hf(t)$ | $T_{DM}$ |
|---|---|---|---|---|---|---|---|---|---|---|---|---|---|---|---|---|
| | | $^{207}Pb/^{206}Pb \pm 1\sigma$ | | $^{207}Pb/^{235}U \pm 1\sigma$ | | $^{206}Pb/^{238}U \pm 1\sigma$ | | $^{207}Pb/^{206}Pb \pm 1\sigma$ | | $^{207}Pb/^{235}U \pm 1\sigma$ | | $^{206}Pb/^{238}U \pm 1\sigma$ | | | | | | | | |
| 09WY-44B-1 | 0.21 | 0.06854 | 0.98 | 1.47419 | 1.79 | 0.15600 | 1.51 | 884.8 | 20.1 | 919.8 | 10.9 | 914.5 | 13.1 | 6.0 | 0.282235 | 0.000010 | 0.002054 | 0.080515 | −0.1 | 1.48 |
| 09WY-44B-2 | 1.10 | 0.06277 | 0.63 | 0.80909 | 1.67 | 0.09348 | 1.55 | 700.6 | 13.4 | 601.9 | 7.6 | 576.1 | 8.5 | −18.6 | 0.282243 | 0.000009 | 0.001448 | 0.058197 | 0.6 | 1.44 |
| 09WY-44B-3 | 0.19 | 0.06853 | 0.98 | 1.46712 | 1.80 | 0.15526 | 1.50 | 884.8 | 20.2 | 916.9 | 10.9 | 930.4 | 13.0 | 5.5 | 0.282128 | 0.000009 | 0.001653 | 0.065279 | −3.6 | 1.61 |
| 09WY-44B-4 | 0.20 | 0.06856 | 1.70 | 1.31257 | 2.30 | 0.13886 | 1.56 | 885.5 | 34.7 | 851.3 | 13.4 | 838.2 | 12.2 | −5.7 | 0.282157 | 0.000010 | 0.001205 | 0.049958 | −2.3 | 1.55 |
| 09WY-44B-5 | 0.14 | 0.06972 | 0.52 | 1.47839 | 1.59 | 0.15378 | 1.50 | 920.2 | 10.7 | 921.6 | 9.7 | 922.1 | 12.9 | 0.2 | 0.282200 | 0.000009 | 0.001900 | 0.078051 | −1.2 | 1.52 |
| 09WY-44B-6 | 0.18 | 0.06963 | 1.06 | 1.45583 | 1.84 | 0.15164 | 1.51 | 917.5 | 21.6 | 912.3 | 11.1 | 910.1 | 12.8 | −0.9 | 0.282177 | 0.000009 | 0.001938 | 0.082936 | −2.1 | 1.55 |
| 09WY-44B-7 | 0.13 | 0.06849 | 0.97 | 1.43758 | 1.78 | 0.15224 | 1.50 | 883.3 | 19.9 | 904.7 | 10.7 | 913.5 | 12.8 | 3.7 | 0.282236 | 0.000009 | 0.002460 | 0.104430 | −0.3 | 1.49 |
| 09WY-44B-8 | 0.14 | 0.06853 | 0.98 | 1.24949 | 1.87 | 0.13224 | 1.59 | 884.5 | 20.1 | 823.2 | 10.6 | 800.6 | 12.0 | −10.1 | 0.282138 | 0.000009 | 0.001665 | 0.065667 | −3.3 | 1.60 |
| 09WY-44B-9 | 0.18 | 0.06948 | 1.27 | 1.47344 | 1.96 | 0.15381 | 1.50 | 912.9 | 25.9 | 919.5 | 11.9 | 922.3 | 12.9 | 1.1 | 0.282179 | 0.000009 | 0.001423 | 0.058977 | −1.7 | 1.53 |
| 09WY-44B-10 | 0.23 | 0.06852 | 0.86 | 1.44807 | 1.74 | 0.15327 | 1.51 | 884.4 | 17.7 | 909.1 | 10.5 | 919.3 | 12.9 | 4.2 | 0.282209 | 0.000009 | 0.001374 | 0.057245 | −0.6 | 1.49 |
| 09WY-44B-11 | 0.14 | 0.06994 | 1.08 | 1.43731 | 1.86 | 0.14905 | 1.51 | 926.6 | 22.1 | 904.6 | 11.2 | 895.6 | 12.7 | −3.6 | 0.282129 | 0.000010 | 0.001421 | 0.059368 | −3.4 | 1.60 |
| 09WY-44B-12 | 0.26 | 0.06996 | 1.36 | 1.46568 | 2.02 | 0.15195 | 1.50 | 927.1 | 27.6 | 916.3 | 12.3 | 911.9 | 12.8 | −1.8 | 0.282160 | 0.000011 | 0.001335 | 0.052058 | −2.3 | 1.55 |
| 09WY-44B-13 | 0.18 | 0.06837 | 1.28 | 1.41539 | 1.97 | 0.15015 | 1.50 | 879.7 | 26.3 | 895.4 | 11.8 | 901.8 | 12.6 | 2.7 | 0.282061 | 0.000010 | 0.001266 | 0.051038 | −5.8 | 1.69 |
| 09WY-44B-14 | 0.29 | 0.06863 | 1.74 | 1.46501 | 2.29 | 0.15482 | 1.50 | 887.6 | 35.5 | 916.1 | 13.9 | 927.9 | 13.0 | 4.9 | 0.282161 | 0.000008 | 0.001410 | 0.053174 | −2.3 | 1.56 |
| 09WY-44B-15 | 0.28 | 0.06884 | 0.91 | 1.44050 | 1.76 | 0.15176 | 1.50 | 894.1 | 18.8 | 905.9 | 10.6 | 910.8 | 12.8 | 2.0 | 0.282303 | 0.000012 | 0.001320 | 0.055779 | 2.8 | 1.35 |
| 09WY-44B-16 | 0.29 | 0.07007 | 1.14 | 1.49250 | 1.88 | 0.15447 | 1.50 | 930.5 | 23.2 | 927.3 | 11.5 | 926.0 | 13.0 | −0.5 | 0.282151 | 0.000027 | 0.000512 | 0.018540 | −2.1 | 1.53 |
| 09WY-44B-17 | 0.30 | 0.07029 | 1.36 | 1.48843 | 2.06 | 0.15357 | 1.55 | 937.0 | 27.6 | 925.7 | 12.6 | 920.9 | 13.3 | −1.8 | 0.282128 | 0.000009 | 0.001722 | 0.069243 | −3.7 | 1.62 |
| 09WY-44B-18 | 0.24 | 0.06836 | 1.17 | 1.45835 | 1.90 | 0.15472 | 1.50 | 879.5 | 24.0 | 913.3 | 11.5 | 927.4 | 13.0 | 5.8 | 0.282113 | 0.000009 | 0.002122 | 0.087635 | −4.4 | 1.65 |
| 09WY-44B-19 | 0.10 | 0.07031 | 1.14 | 1.49050 | 2.02 | 0.15376 | 1.67 | 937.3 | 23.1 | 926.5 | 12.3 | 922.0 | 14.3 | −1.7 | 0.282096 | 0.000009 | 0.001460 | 0.055030 | −4.6 | 1.65 |
| 09WY-44B-20 | 0.18 | 0.06889 | 0.81 | 1.40771 | 1.71 | 0.14821 | 1.50 | 895.4 | 16.6 | 892.2 | 10.2 | 890.9 | 12.5 | −0.5 | 0.282161 | 0.000009 | 0.001671 | 0.070216 | −2.5 | 1.57 |
| 09WY-44B-22 | 0.29 | 0.06676 | 5.59 | 1.46062 | 5.79 | 0.15868 | 1.52 | 830.3 | 112.3 | 914.3 | 35.5 | 919.4 | 13.4 | 15.4 | | | | | | |
| 09WY-44B-23 | 0.27 | 0.06881 | 1.50 | 1.32824 | 2.30 | 0.13999 | 1.75 | 893.1 | 30.7 | 858.1 | 13.4 | 844.6 | 13.8 | −5.8 | | | | | | |
| 09WY-44B-24 | 0.23 | 0.06795 | 1.69 | 1.46379 | 2.26 | 0.15623 | 1.50 | 867.1 | 34.6 | 915.6 | 13.7 | 935.8 | 13.1 | 8.5 | | | | | | |
| 09WY-44B-25 | 0.24 | 0.06982 | 1.15 | 1.47442 | 1.89 | 0.15315 | 1.50 | 923.2 | 23.5 | 919.9 | 11.5 | 918.6 | 12.9 | −0.5 | | | | | | |

**Table 2**
LA-ICPMS zircon U–Pb and Lu–Hf analytical result of early Neoproterozoic granitic gneisses from Wuyi-Yunkai, Cathaysia Block.

| spot | Th/U | Isotopic ratios | | | | Apparent age (Ma) | | | | | | | | $^{176}Hf/^{177}Hf$ | | $^{176}Lu/^{177}Hf$ | $^{176}Yb/^{177}Hf$ | εHf(t) | $T_{DM}$ |
|---|---|---|---|---|---|---|---|---|---|---|---|---|---|---|---|---|---|---|---|
| | | $^{207}Pb/^{206}Pb \pm 1\sigma$ | | $^{207}Pb/^{235}U \pm 1\sigma$ | | $^{206}Pb/^{238}U \pm 1\sigma$ | | $^{207}Pb/^{206}Pb \pm 1\sigma$ | | $^{207}Pb/^{235}U \pm 1\sigma$ | | $^{206}Pb/^{238}U \pm 1\sigma$ | | | | | | | |
| 09WG-44A granitic gneiss from Masha, Jianyang, Wuyi Mountain | | | | | | | | | | | | | | | | | | | |
| 09WG-44A-1 | 0.51 | 0.06983 | 0.00175 | 1.46546 | 0.03768 | 0.15221 | 0.00391 | 913 | 22 | 916 | 16 | 924 | 51 | 0.282208 | 0.000019 | 0.001592 | 0.050774 | −0.8 | 1.50 |
| 09WG-44A-2 | 0.23 | 0.06776 | 0.0017 | 1.3844 | 0.03513 | 0.14815 | 0.00374 | 891 | 21 | 882 | 15 | 861 | 56 | 0.282235 | 0.000018 | 0.001297 | 0.040428 | 0.4 | 1.45 |
| 09WG-44A-3 | 0.17 | 0.06897 | 0.00173 | 1.43471 | 0.03708 | 0.15087 | 0.0039 | 906 | 22 | 904 | 15 | 898 | 47 | 0.282176 | 0.000022 | 0.002050 | 0.059871 | −2.2 | 1.56 |
| 09WG-44A-4 | 0.58 | 0.06928 | 0.00173 | 1.45423 | 0.03724 | 0.15225 | 0.0039 | 914 | 22 | 912 | 15 | 907 | 56 | 0.282188 | 0.000021 | 0.001821 | 0.057239 | −1.6 | 1.54 |
| 09WG-44A-5 | 0.35 | 0.06884 | 0.00172 | 1.44699 | 0.03668 | 0.15243 | 0.00386 | 915 | 22 | 909 | 15 | 894 | 52 | 0.282251 | 0.000020 | 0.002582 | 0.077587 | 0.2 | 1.48 |
| 09WG-44A-6 | 0.48 | 0.06906 | 0.00173 | 1.44458 | 0.03663 | 0.1517 | 0.00384 | 910 | 22 | 908 | 15 | 902 | 52 | 0.282147 | 0.000021 | 0.002079 | 0.062418 | −3.2 | 1.60 |
| 09WG-44A-7 | 0.22 | 0.06899 | 0.00173 | 1.43776 | 0.03663 | 0.15113 | 0.00385 | 907 | 22 | 905 | 15 | 898 | 47 | 0.282082 | 0.000019 | 0.001563 | 0.044193 | −5.2 | 1.67 |
| 09WG-44A-8 | 0.05 | 0.06826 | 0.00172 | 1.40404 | 0.0357 | 0.14914 | 0.00376 | 896 | 21 | 891 | 15 | 876 | 47 | 0.282150 | 0.000019 | 0.002082 | 0.062126 | −3.1 | 1.60 |
| 09WG-44A-9 | 0.21 | 0.07045 | 0.00177 | 1.47734 | 0.03746 | 0.15207 | 0.00384 | 913 | 22 | 921 | 15 | 943 | 46 | 0.282177 | 0.000019 | 0.002799 | 0.083640 | −2.6 | 1.59 |
| 09WG-44A-10 | 0.38 | 0.06879 | 0.00172 | 1.44164 | 0.03737 | 0.15195 | 0.00393 | 912 | 22 | 906 | 16 | 892 | 52 | 0.282163 | 0.000021 | 0.001904 | 0.057543 | −2.5 | 1.57 |
| 09WG-44A-11 | 0.08 | 0.06562 | 0.00165 | 1.05805 | 0.02775 | 0.11669 | 0.00299 | 711 | 17 | 733 | 14 | 794 | 58 | 0.282172 | 0.000016 | 0.001313 | 0.039838 | −1.9 | 1.54 |
| 09WG-44A-12 | 0.02 | 0.06768 | 0.0017 | 1.22489 | 0.03187 | 0.1311 | 0.00337 | 794 | 19 | 812 | 15 | 859 | 52 | 0.282259 | 0.000018 | 0.002537 | 0.076271 | 0.5 | 1.46 |
| 09WG-44A-13 | 0.11 | 0.06853 | 0.00172 | 1.43081 | 0.03705 | 0.15142 | 0.00392 | 909 | 22 | 902 | 15 | 885 | 84 | 0.282206 | 0.000024 | 0.001731 | 0.050468 | −0.9 | 1.50 |
| 09WG-44A-14 | 0.07 | 0.06882 | 0.00172 | 1.43951 | 0.03676 | 0.15169 | 0.00387 | 910 | 22 | 906 | 15 | 894 | 52 | 0.282201 | 0.000017 | 0.001687 | 0.053879 | −1.1 | 1.51 |
| 09WG-44A-15 | 0.13 | 0.0689 | 0.00173 | 1.43336 | 0.03687 | 0.15085 | 0.00388 | 906 | 22 | 903 | 15 | 895 | 52 | 0.282168 | 0.000017 | 0.000781 | 0.025221 | −1.7 | 1.52 |
| 09WG-44A-16 | 0.44 | 0.06869 | 0.00172 | 1.26063 | 0.0342 | 0.13295 | 0.00354 | 805 | 20 | 828 | 15 | 900 | 52 | 0.282184 | 0.000024 | 0.002051 | 0.059437 | −1.9 | 1.55 |
| 09WG-44A-17 | 0.05 | 0.06892 | 0.00173 | 1.43787 | 0.03652 | 0.15125 | 0.00382 | 908 | 21 | 905 | 15 | 898 | 52 | 0.282186 | 0.000019 | 0.002943 | 0.087153 | −2.4 | 1.58 |
| 09WG-44A-18 | 0.07 | 0.06828 | 0.00171 | 1.27342 | 0.03318 | 0.13506 | 0.00347 | 817 | 20 | 834 | 15 | 876 | 47 | 0.282159 | 0.000020 | 0.001754 | 0.052975 | −2.6 | 1.57 |
| 09WG-44A-19 | 0.38 | 0.06896 | 0.00173 | 1.43798 | 0.03685 | 0.15122 | 0.00387 | 908 | 22 | 905 | 15 | 898 | 47 | 0.282163 | 0.000018 | 0.002149 | 0.064733 | −2.7 | 1.58 |
| 09WG-44A-20 | 0.16 | 0.06999 | 0.00176 | 1.46694 | 0.03713 | 0.15198 | 0.00383 | 912 | 21 | 917 | 15 | 928 | 56 | 0.282102 | 0.000019 | 0.001272 | 0.036847 | −4.3 | 1.63 |
| 09WG-44A-21 | 0.18 | 0.06915 | 0.00173 | 1.4409 | 0.03677 | 0.15111 | 0.00385 | 907 | 22 | 906 | 15 | 903 | 52 | 0.282107 | 0.000022 | 0.001735 | 0.047255 | −4.4 | 1.65 |
| 09WG-44A-22 | 0.56 | 0.06793 | 0.0017 | 1.23222 | 0.03126 | 0.13152 | 0.00332 | 797 | 19 | 815 | 14 | 866 | 52 | 0.282284 | 0.000023 | 0.002592 | 0.081424 | 1.3 | 1.43 |
| 09WG-44A-23 | 0.2 | 0.06888 | 0.00173 | 1.4479 | 0.03787 | 0.15245 | 0.00399 | 915 | 22 | 909 | 16 | 894 | 52 | 0.282166 | 0.000018 | 0.001347 | 0.040311 | −2.1 | 1.55 |
| 09WG-44A-24 | 0.15 | 0.06884 | 0.00173 | 1.44632 | 0.0395 | 0.15223 | 0.00413 | 913 | 23 | 908 | 16 | 894 | 52 | 0.282087 | 0.000017 | 0.001285 | 0.038856 | −4.9 | 1.65 |
| 09WG-44A-25 | 0.72 | 0.06887 | 0.00172 | 1.43082 | 0.03685 | 0.15066 | 0.00388 | 905 | 22 | 902 | 15 | 894 | 52 | 0.282227 | 0.000023 | 0.002424 | 0.077467 | −0.6 | 1.50 |
| 12WY-116C granitic gneiss from Hezi, Anyuan, Nanling Mountain | | | | | | | | | | | | | | | | | | | |
| 12WY-116C-01 | 0.54 | 0.069933 | 0.002068 | 1.287489 | 0.046393 | 0.132096 | 0.003460 | 928 | 61 | 840 | 21 | 800 | 20 | 0.281900 | 0.000049 | 0.000677 | 0.016021 | −9.6 | 1.89 |
| 12WY-116C-02 | 0.40 | 0.114766 | 0.002876 | 5.458031 | 0.138518 | 0.344795 | 0.008742 | 1876 | 45 | 1894 | 22 | 1910 | 42 | 0.281594 | 0.000028 | 0.001550 | 0.036625 | −1.1 | 2.36 |
| 12WY-116C-03 | 1.05 | 0.163449 | 0.004094 | 9.977553 | 0.252126 | 0.442584 | 0.011178 | 2492 | 42 | 2433 | 23 | 2362 | 50 | 0.281216 | 0.000017 | 0.000466 | 0.010931 | −2.9 | 2.80 |
| 12WY-116C-04 | 0.56 | 0.076874 | 0.001953 | 1.741020 | 0.044347 | 0.164267 | 0.004246 | 1118 | 51 | 1024 | 16 | 980 | 24 | 0.281918 | 0.000027 | 0.000623 | 0.015351 | −9.0 | 1.86 |
| 12WY-116C-05 | 0.39 | 0.070899 | 0.001777 | 1.615065 | 0.041317 | 0.165169 | 0.004223 | 954 | 52 | 976 | 16 | 985 | 23 | 0.282165 | 0.000027 | 0.000518 | 0.012629 | 0.0 | 1.51 |
| 12WY-116C-06 | 0.70 | 0.165521 | 0.004147 | 11.02025 | 0.280495 | 0.482665 | 0.012265 | 2513 | 42 | 2525 | 24 | 2539 | 53 | 0.281210 | 0.000028 | 0.000494 | 0.011299 | 0.9 | 2.81 |
| 12WY-116C-07 | 0.54 | 0.090386 | 0.002272 | 3.112952 | 0.079227 | 0.249672 | 0.006322 | 1435 | 48 | 1436 | 20 | 1437 | 33 | 0.281614 | 0.000025 | 0.000376 | 0.009303 | −9.5 | 2.26 |
| 12WY-116C-10 | 0.18 | 0.070895 | 0.001776 | 1.604322 | 0.040636 | 0.164056 | 0.004150 | 954 | 52 | 972 | 16 | 979 | 23 | 0.282073 | 0.000024 | 0.000297 | 0.007902 | −3.3 | 1.63 |
| 12WY-116C-11 | 0.57 | 0.071760 | 0.001799 | 1.630321 | 0.041866 | 0.164776 | 0.004236 | 989 | 51 | 982 | 16 | 983 | 23 | 0.281927 | 0.000019 | 0.000517 | 0.013000 | −8.5 | 1.84 |
| 12WY-116C-12 | 0.37 | 0.070437 | 0.001767 | 1.590317 | 0.041239 | 0.163631 | 0.004219 | 943 | 51 | 966 | 16 | 977 | 23 | 0.282201 | 0.000026 | 0.000861 | 0.019470 | 0.8 | 1.48 |
| 12WY-116C-13 | 0.22 | 0.103587 | 0.002602 | 4.303276 | 0.109601 | 0.301454 | 0.007714 | 1700 | 79 | 1694 | 21 | 1699 | 38 | 0.281714 | 0.000020 | 0.001126 | 0.026966 | −0.9 | 2.17 |
| 12WY-116C-14 | 0.18 | 0.179993 | 0.004514 | 12.53618 | 0.335357 | 0.504212 | 0.013320 | 2653 | 41 | 2645 | 25 | 2632 | 57 | 0.281361 | 0.000022 | 0.000674 | 0.016763 | 8.0 | 2.62 |
| 12WY-116C-15 | 0.31 | 0.178526 | 0.004477 | 12.48813 | 0.337850 | 0.507011 | 0.013676 | 2639 | 41 | 2642 | 25 | 2644 | 59 | 0.281210 | 0.000027 | 0.000671 | 0.015633 | 2.9 | 2.82 |
| 12WY-116C-16 | 0.56 | 0.075904 | 0.001910 | 1.732341 | 0.044780 | 0.165474 | 0.004274 | 1092 | 50 | 1021 | 17 | 987 | 24 | 0.281919 | 0.000026 | 0.000640 | 0.014922 | −8.8 | 1.86 |
| 12WY-116C-17 | 0.48 | 0.088644 | 0.002225 | 2.997010 | 0.076070 | 0.245142 | 0.006211 | 1398 | 48 | 1407 | 19 | 1413 | 32 | 0.282128 | 0.000031 | 0.001089 | 0.025998 | 7.6 | 1.59 |
| 12WY-116C-18 | 0.63 | 0.135501 | 0.003402 | 7.339980 | 0.188746 | 0.392621 | 0.010013 | 2172 | 43 | 2154 | 23 | 2135 | 46 | 0.281804 | 0.000031 | 0.000722 | 0.015956 | 12.5 | 2.02 |
| 12WY-116C-19 | 0.20 | 0.072610 | 0.001821 | 1.645784 | 0.042068 | 0.164409 | 0.004217 | 1003 | 51 | 988 | 16 | 981 | 23 | 0.281988 | 0.000031 | 0.000645 | 0.016361 | −6.5 | 1.76 |
| 12WY-116C-20 | 0.41 | 0.099812 | 0.002503 | 3.891745 | 0.098597 | 0.282663 | 0.007148 | 1621 | 47 | 1612 | 20 | 1605 | 36 | 0.281738 | 0.000028 | 0.000352 | 0.007719 | −1.3 | 2.09 |
| 12WY-116C-21 | 0.68 | 0.072116 | 0.001808 | 1.629254 | 0.041810 | 0.163779 | 0.004197 | 991 | 50 | 982 | 16 | 978 | 23 | 0.282147 | 0.000029 | 0.000755 | 0.020330 | −1.0 | 1.55 |
| 12WY-116C-22 | 1.60 | 0.072883 | 0.001838 | 1.656724 | 0.042901 | 0.164818 | 0.004247 | 1011 | 51 | 992 | 16 | 983 | 24 | 0.282114 | 0.000029 | 0.000714 | 0.019969 | −2.0 | 1.59 |
| 12WY-116C-23 | 0.55 | 0.091082 | 0.002282 | 3.163404 | 0.084007 | 0.251766 | 0.006678 | 1450 | 48 | 1448 | 20 | 1448 | 34 | 0.282072 | 0.000028 | 0.000412 | 0.010441 | 7.0 | 1.64 |
| 12WY-116C-25 | 0.48 | 0.065461 | 0.001737 | 0.917715 | 0.024018 | 0.101860 | 0.002632 | 791 | 56 | 661 | 13 | 625 | 15 | 0.282054 | 0.000031 | 0.000378 | 0.010404 | −4.0 | 1.66 |
| 12WY-116C-26 | 0.17 | 0.092182 | 0.002311 | 3.008877 | 0.076406 | 0.236595 | 0.005992 | 1472 | 42 | 1410 | 19 | 1369 | 31 | 0.282158 | 0.000033 | 0.001519 | 0.042537 | 7.3 | 1.56 |
| 12WY-116C-27 | 0.14 | 0.072216 | 0.001810 | 1.634480 | 0.042112 | 0.164076 | 0.004222 | 992 | 51 | 984 | 16 | 979 | 23 | 0.282111 | 0.000040 | 0.000560 | 0.014462 | −2.1 | 1.59 |
| 12WY-116C-29 | 0.22 | 0.065003 | 0.001713 | 0.916051 | 0.024036 | 0.102242 | 0.002609 | 776 | 56 | 660 | 13 | 628 | 15 | 0.281898 | 0.000047 | 0.000405 | 0.011096 | −9.5 | 1.87 |
| 12WY-116C-30 | 0.07 | 0.067433 | 0.001693 | 1.046782 | 0.026686 | 0.112542 | 0.002865 | 850 | 52 | 727 | 13 | 687 | 17 | 0.281973 | 0.000024 | 0.000555 | 0.014786 | −7.0 | 1.78 |

**Table 2** (*Continued*)

| spot | Th/U | Isotopic ratios | | | | Apparent age (Ma) | | | | | | | | $^{176}Hf/^{177}Hf$ | | $^{176}Lu/^{177}Hf$ | $^{176}Yb/^{177}Hf$ | εHf(t) | $T_{DM}$ |
|---|---|---|---|---|---|---|---|---|---|---|---|---|---|---|---|---|---|---|---|
| | | $^{207}Pb/^{206}Pb \pm 1\sigma$ | | $^{207}Pb/^{235}U \pm 1\sigma$ | | $^{206}Pb/^{238}U \pm 1\sigma$ | | $^{207}Pb/^{206}Pb \pm 1\sigma$ | | $^{207}Pb/^{235}U \pm 1\sigma$ | | $^{206}Pb/^{238}U \pm 1\sigma$ | | | | | | | |
| 12WY-118A granitic gneiss from Hezi, Anyuan, Nanling Mountain | | | | | | | | | | | | | | | | | | | |
| 12WY-118A-01 | 0.50 | 0.082741 | 0.002333 | 2.265658 | 0.064757 | 0.198591 | 0.005641 | 1265 | 55 | 1202 | 20 | 1168 | 30 | 0.282176 | 0.000014 | 0.001129 | 0.032194 | 3.9 | 1.52 |
| 12WY-118A-03 | 1.02 | 0.084498 | 0.002370 | 2.577412 | 0.073763 | 0.221228 | 0.006327 | 1306 | 58 | 1294 | 21 | 1288 | 33 | 0.282127 | 0.000023 | 0.001201 | 0.030235 | 4.7 | 1.59 |
| 12WY-118A-04 | 0.29 | 0.069736 | 0.001968 | 1.564159 | 0.044560 | 0.162650 | 0.004598 | 920 | 58 | 956 | 18 | 971 | 25 | 0.282137 | 0.000025 | 0.000505 | 0.014163 | −1.3 | 1.55 |
| 12WY-118A-06 | 0.47 | 0.071032 | 0.002002 | 1.591090 | 0.045708 | 0.162446 | 0.004642 | 967 | 58 | 967 | 18 | 970 | 26 | 0.281974 | 0.000025 | 0.000535 | 0.014672 | −7.1 | 1.78 |
| 12WY-118A-07 | 0.45 | 0.070995 | 0.001994 | 1.602940 | 0.046804 | 0.163724 | 0.004772 | 967 | 57 | 971 | 18 | 977 | 26 | 0.281976 | 0.000025 | 0.000570 | 0.014667 | −6.9 | 1.78 |
| 12WY-118A-08 | 0.56 | 0.072434 | 0.002035 | 1.643495 | 0.047243 | 0.164534 | 0.004718 | 998 | 57 | 987 | 18 | 982 | 26 | 0.282149 | 0.000020 | 0.000436 | 0.011382 | −0.6 | 1.53 |
| 12WY-118A-09 | 0.41 | 0.072807 | 0.002056 | 1.665107 | 0.051557 | 0.165093 | 0.004979 | 1009 | 57 | 995 | 20 | 985 | 28 | 0.281988 | 0.000024 | 0.000734 | 0.020842 | −6.5 | 1.77 |
| 12WY-118A-10 | 0.57 | 0.073661 | 0.002072 | 1.673708 | 0.047513 | 0.164754 | 0.004663 | 1031 | 56 | 999 | 18 | 983 | 26 | 0.281970 | 0.000024 | 0.001669 | 0.046639 | −7.7 | 1.84 |
| 12WY-118A-11 | 0.40 | 0.073320 | 0.002060 | 1.669010 | 0.047475 | 0.165167 | 0.004708 | 1033 | 57 | 997 | 18 | 985 | 26 | 0.282125 | 0.000027 | 0.001129 | 0.029834 | −1.9 | 1.59 |
| 12WY-118A-12 | 0.12 | 0.121065 | 0.003396 | 5.778777 | 0.163137 | 0.346202 | 0.009782 | 1972 | 50 | 1943 | 24 | 1916 | 47 | 0.281821 | 0.000023 | 0.000738 | 0.017346 | 8.2 | 2.00 |
| 12WY-118A-13 | 0.32 | 0.076362 | 0.002183 | 1.732794 | 0.061283 | 0.163241 | 0.005398 | 1106 | 53 | 1021 | 23 | 975 | 30 | 0.282125 | 0.000016 | 0.001998 | 0.052978 | −2.6 | 1.63 |
| 12WY-118A-14 | 0.37 | 0.065227 | 0.001880 | 0.933234 | 0.027483 | 0.103733 | 0.002975 | 783 | 61 | 669 | 14 | 636 | 17 | 0.282088 | 0.000031 | 0.001080 | 0.025805 | −3.4 | 1.64 |
| 12WY-118A-15 | 0.42 | 0.075211 | 0.002114 | 1.690981 | 0.048400 | 0.163074 | 0.004666 | 1076 | 56 | 1005 | 18 | 974 | 26 | 0.282128 | 0.000027 | 0.000974 | 0.026479 | −1.9 | 1.58 |
| 12WY-118A-16 | 0.61 | 0.077653 | 0.002229 | 1.788852 | 0.051562 | 0.167137 | 0.004748 | 1139 | 57 | 1041 | 19 | 996 | 26 | 0.282088 | 0.000025 | 0.000590 | 0.016050 | −2.6 | 1.62 |
| 12WY-118A-18 | 0.24 | 0.066523 | 0.001874 | 0.983955 | 0.029079 | 0.107135 | 0.003102 | 833 | 58 | 696 | 15 | 656 | 18 | 0.282182 | 0.000030 | 0.000391 | 0.010526 | 0.4 | 1.49 |
| 12WY-118A-19 | 0.40 | 0.070131 | 0.001973 | 1.565155 | 0.044628 | 0.161817 | 0.004595 | 931 | 58 | 957 | 18 | 967 | 25 | 0.282069 | 0.000045 | 0.001947 | 0.048728 | −4.8 | 1.71 |
| 12WY-118A-20 | 0.60 | 0.072229 | 0.002052 | 1.654980 | 0.047945 | 0.166261 | 0.004777 | 992 | 25 | 991 | 18 | 991 | 26 | 0.282163 | 0.000032 | 0.001045 | 0.028798 | −0.3 | 1.54 |
| 12WY-118A-21 | 1.59 | 0.076004 | 0.002137 | 1.754912 | 0.049935 | 0.167483 | 0.004772 | 1094 | 56 | 1029 | 18 | 998 | 26 | 0.282153 | 0.000024 | 0.000573 | 0.015154 | −0.2 | 1.53 |
| 12WY-118A-22 | 0.90 | 0.067074 | 0.001912 | 1.117679 | 0.034928 | 0.120139 | 0.003568 | 839 | 55 | 762 | 17 | 731 | 21 | 0.282122 | 0.000021 | 0.000756 | 0.020294 | −1.9 | 1.58 |
| 12WY-118A-23 | 0.63 | 0.074107 | 0.002090 | 1.707550 | 0.048871 | 0.167157 | 0.004788 | 1044 | 57 | 1011 | 18 | 996 | 26 | | | | | | |
| 12WY-118A-24 | 0.51 | 0.128231 | 0.003599 | 6.592510 | 0.190614 | 0.372702 | 0.010746 | 2074 | 45 | 2058 | 25 | 2042 | 50 | | | | | | |
| 12WY-118A-25 | 0.42 | 0.074794 | 0.002098 | 1.717778 | 0.050814 | 0.166523 | 0.004916 | 1065 | 56 | 1015 | 19 | 993 | 27 | | | | | | |
| 12WY-118A-26 | 0.63 | 0.069271 | 0.001945 | 1.558507 | 0.044096 | 0.163134 | 0.004603 | 907 | 58 | 954 | 18 | 974 | 26 | | | | | | |
| 12WY-118A-27 | 0.52 | 0.073639 | 0.002086 | 1.679154 | 0.048064 | 0.165668 | 0.004766 | 1031 | 57 | 1001 | 18 | 988 | 26 | | | | | | |
| 12WY-118A-28 | 0.42 | 0.073401 | 0.002061 | 1.649340 | 0.046895 | 0.162957 | 0.004624 | 1025 | 56 | 989 | 18 | 973 | 26 | | | | | | |
| 12WY-118A-29 | 0.13 | 0.066317 | 0.001865 | 1.036571 | 0.032897 | 0.113216 | 0.003537 | 817 | 55 | 722 | 16 | 691 | 20 | | | | | | |
| 12WY-118A-30 | 0.50 | 0.065075 | 0.002373 | 0.922263 | 0.040580 | 0.101863 | 0.002999 | 776 | 77 | 664 | 21 | 625 | 18 | | | | | | |
| 12YK-58C gneissic granite from Longxin, Luoding, Yunkai Mountain | | | | | | | | | | | | | | | | | | | |
| 12YK-58C-02 | 0.74 | 0.065374 | 0.001641 | 1.025407 | 0.028170 | 0.113659 | 0.003098 | 787 | 54 | 717 | 14 | 694 | 18 | | | | | | |
| 12YK-58C-03 | 0.67 | 0.066567 | 0.001670 | 0.901702 | 0.022865 | 0.098195 | 0.002483 | 833 | 52 | 653 | 12 | 604 | 15 | | | | | | |
| 12YK-58C-04 | 0.60 | 0.064791 | 0.001630 | 0.902353 | 0.022994 | 0.100960 | 0.002559 | 769 | 49 | 653 | 12 | 620 | 15 | | | | | | |
| 12YK-58C-06 | 0.75 | 0.069962 | 0.001771 | 1.387316 | 0.035674 | 0.143738 | 0.003650 | 928 | 56 | 884 | 15 | 866 | 21 | | | | | | |
| 12YK-58C-07 | 0.54 | 0.067784 | 0.001703 | 1.142847 | 0.029708 | 0.122188 | 0.003147 | 861 | 56 | 774 | 14 | 743 | 18 | | | | | | |
| 12YK-58C-08 | 1.21 | 0.124310 | 0.003118 | 5.615209 | 0.142301 | 0.327466 | 0.008287 | 2020 | 44 | 1918 | 22 | 1826 | 40 | | | | | | |
| 12YK-58C-09 | 1.05 | 0.065665 | 0.001661 | 1.118304 | 0.030498 | 0.123475 | 0.003342 | 794 | 53 | 762 | 15 | 751 | 19 | 0.282020 | 0.000026 | 0.000963 | 0.026049 | −6.8 | 1.73 |
| 12YK-58C-10 | 0.93 | 0.122158 | 0.003067 | 4.985237 | 0.131315 | 0.295770 | 0.007744 | 1988 | 44 | 1817 | 22 | 1670 | 39 | 0.281855 | 0.000042 | 0.001697 | 0.037428 | 2.8 | 2.00 |
| 12YK-58C-11 | 0.85 | 0.066380 | 0.001685 | 0.934800 | 0.024128 | 0.102074 | 0.002585 | 818 | 54 | 670 | 13 | 627 | 15 | 0.282012 | 0.000027 | 0.001057 | 0.025826 | −7.1 | 1.75 |
| 12YK-58C-12 | 1.31 | 0.123859 | 0.003117 | 6.192258 | 0.158907 | 0.362501 | 0.009275 | 2013 | 44 | 2003 | 22 | 1994 | 44 | 0.281806 | 0.000053 | 0.00075 | 0.018512 | 9.4 | 2.02 |
| 12YK-58C-13 | 0.75 | 0.069980 | 0.001757 | 1.334190 | 0.034428 | 0.138215 | 0.003552 | 928 | 56 | 861 | 15 | 835 | 20 | | | | | | |
| 12YK-58C-16 | 0.61 | 0.122625 | 0.003080 | 4.657135 | 0.129422 | 0.274903 | 0.007461 | 1995 | 44 | 1760 | 23 | 1566 | 38 | 0.282063 | 0.000057 | 0.001251 | 0.03091 | 8.4 | 1.69 |
| 12YK-58C-17 | 0.26 | 0.066711 | 0.001675 | 1.032656 | 0.026328 | 0.112233 | 0.002852 | 828 | 52 | 720 | 13 | 686 | 17 | 0.282055 | 0.000060 | 0.00095 | 0.022426 | −5.5 | 1.68 |
| 12YK-58C-18 | 1.26 | 0.068965 | 0.001749 | 1.355514 | 0.035162 | 0.142477 | 0.003629 | 898 | 47 | 870 | 15 | 859 | 20 | 0.282019 | 0.000069 | 0.000902 | 0.022805 | −6.7 | 1.73 |
| 12YK-58C-19 | 0.58 | 0.064320 | 0.001638 | 0.898181 | 0.024432 | 0.101285 | 0.002743 | 754 | 54 | 651 | 13 | 622 | 16 | 0.282020 | 0.000075 | 0.000941 | 0.022745 | −6.7 | 1.73 |
| 12YK-58C-20 | 1.18 | 0.065335 | 0.001648 | 1.032482 | 0.026362 | 0.114583 | 0.002905 | 785 | 54 | 720 | 13 | 699 | 17 | 0.282018 | 0.000040 | 0.001123 | 0.027609 | −6.9 | 1.74 |
| 12YK-58C-21 | 0.43 | 0.067311 | 0.001690 | 1.272043 | 0.032857 | 0.137017 | 0.003526 | 856 | 52 | 833 | 15 | 828 | 20 | 0.281998 | 0.000061 | 0.000546 | 0.014048 | −7.3 | 1.74 |
| 12YK-58C-22 | 0.86 | 0.067727 | 0.001720 | 1.173315 | 0.030124 | 0.125629 | 0.003196 | 861 | 58 | 788 | 14 | 763 | 18 | 0.282020 | 0.000036 | 0.001005 | 0.024028 | −6.8 | 1.74 |
| 12YK-58C-23 | 0.68 | 0.064234 | 0.001611 | 0.892774 | 0.022650 | 0.100765 | 0.002549 | 750 | 253 | 648 | 12 | 619 | 15 | | | | | | |
| 12YK-58C-25 | 0.87 | 0.068070 | 0.001732 | 1.115323 | 0.029239 | 0.118868 | 0.003121 | 872 | 54 | 761 | 14 | 724 | 18 | 0.282019 | 0.000047 | 0.001569 | 0.037984 | −7.2 | 1.76 |
| 12YK-58C-26 | 1.00 | 0.124130 | 0.003112 | 6.210428 | 0.157723 | 0.362729 | 0.009197 | 2016 | 44 | 2006 | 22 | 1995 | 44 | 0.281817 | 0.000021 | 0.001091 | 0.028395 | 9.3 | 2.02 |
| 12YK-58C-27 | 1.24 | 0.125445 | 0.003146 | 6.256098 | 0.159873 | 0.361551 | 0.009216 | 2035 | 44 | 2012 | 22 | 1990 | 44 | 0.281866 | 0.000039 | 0.001051 | 0.025383 | 11.0 | 1.95 |
| 12YK-58C-28 | 0.14 | 0.119681 | 0.003011 | 4.251242 | 0.117369 | 0.257160 | 0.006952 | 1952 | 45 | 1684 | 23 | 1475 | 36 | | | | | | |
| 12YK-58C-29 | 0.57 | 0.068810 | 0.001730 | 1.398938 | 0.035629 | 0.147405 | 0.003746 | 894 | 52 | 888 | 15 | 886 | 21 | | | | | | |
| 12YK-58C-30 | 1.34 | 0.064972 | 0.001635 | 0.887964 | 0.022964 | 0.099092 | 0.002560 | 772 | 53 | 645 | 12 | 609 | 15 | | | | | | |

| | | | | | | | | | | | | | | | |
|---|---|---|---|---|---|---|---|---|---|---|---|---|---|---|---|
| 09YK-6A gneissic granite from Huaixiang, Xinyi, Yunkai Mountain | | | | | | | | | | | | | | | |
| 09YK-6A-1 | 0.53 | 0.112505 | 0.002210 | 5.095362 | 0.098789 | 0.328474 | 0.006284 | 1840 | 35 | 1835 | 16 | 1831 | 30 | | |
| 09YK-6A-2 | 0.91 | 0.072225 | 0.001520 | 1.621069 | 0.034408 | 0.162785 | 0.003484 | 992 | 42 | 978 | 13 | 972 | 19 | | |
| 09YK-6A-3 | 0.49 | 0.168358 | 0.003541 | 10.75271 | 0.233001 | 0.463217 | 0.010323 | 2541 | 35 | 2502 | 20 | 2454 | 45 | | |
| 09YK-6A-4 | 0.99 | 0.070566 | 0.001487 | 1.575549 | 0.033535 | 0.161933 | 0.003481 | 945 | 43 | 961 | 13 | 968 | 19 | | |
| 09YK-6A-5 | 0.62 | 0.070858 | 0.001493 | 1.520673 | 0.032524 | 0.155650 | 0.003377 | 953 | 43 | 939 | 13 | 933 | 19 | | |
| 09YK-6A-6 | 0.19 | 0.070682 | 0.001990 | 1.553859 | 0.037889 | 0.159441 | 0.003173 | 948 | 57 | 952 | 15 | 954 | 18 | | |
| 09YK-6A-7 | 1.26 | 0.074989 | 0.001717 | 1.842116 | 0.041780 | 0.178164 | 0.004002 | 1068 | 45 | 1061 | 15 | 1057 | 22 | | |
| 09YK-6A-8 | 0.17 | 0.068243 | 0.001437 | 1.483121 | 0.032003 | 0.157622 | 0.003480 | 876 | 43 | 924 | 13 | 944 | 19 | | |
| 09YK-6A-10 | 0.96 | 0.072900 | 0.001679 | 1.555002 | 0.035753 | 0.154705 | 0.003552 | 1011 | 46 | 952 | 14 | 927 | 20 | | |
| 09YK-6A-11 | 0.68 | 0.171590 | 0.003613 | 11.74902 | 0.252926 | 0.496603 | 0.010921 | 2573 | 35 | 2585 | 20 | 2599 | 47 | | |
| 09YK-6A-12 | 0.61 | 0.157678 | 0.003353 | 9.928543 | 0.218571 | 0.456681 | 0.010386 | 2431 | 36 | 2428 | 20 | 2425 | 46 | | |
| 09YK-6A-13 | 0.40 | 0.070742 | 0.001495 | 1.594628 | 0.034013 | 0.163487 | 0.003518 | 950 | 43 | 968 | 13 | 976 | 19 | | |
| 09YK-6A-14 | 0.51 | 0.113491 | 0.002395 | 5.099724 | 0.108075 | 0.325900 | 0.006935 | 1856 | 38 | 1836 | 18 | 1818 | 34 | | |
| 09YK-6A-15 | 0.52 | 0.115273 | 0.002423 | 5.121257 | 0.108292 | 0.322216 | 0.006853 | 1884 | 37 | 1840 | 18 | 1801 | 33 | | |

*Notes*: $\varepsilon$Hf(t) values and $T_{DM}$ for grains with the UPb age of younger than 1000 Ma from 09WG-44A, 12WY-116C, 12WY-118A and 12YK-58C are back-calculated to the formation ages of 913 Ma, 982 Ma, 963 Ma and 926 Ma, respectively.

Seven out of 13 grains from 09YK-6A show Th/U ratios of 0.17–0.99 and give weighted mean age of 954 ± 14 Ma with MSWD = 1.0 (Fig. 6b). The $^{206}Pb/^{207}Pb$ apparent ages of the remaining six grains for 09YK-6A cluster at 1840–1884 Ma ($n$ = 3) and 2431–2573 Ma ($n$ = 3), respectively.

## 5. Whole-rock geochemical results

The elemental and Sr–Nd isotopic analytical results for the representative samples are presented in Table 4. These samples exhibit $SiO_2$ = 65.6–77.2 wt%, $Al_2O_3$ = 11.3–16.6 wt%, FeOt = 4.3–6.6 wt%, MgO = 0.89–3.39 wt%, CaO = 1.33–2.88 wt % and $K_2O + Na_2O$ = 4.0–7.2 wt %. $TiO_2$ contents range from 0.44 wt% to 0.91 wt % and $P_2O_5$ from 0.05 wt% to 0.18 wt%. They show high $TiO_2$ + FeOt + MgO (5.8–10.2 wt%) and $Al_2O_3/(Na_2O + CaO)$ ratios (2.36–4.28). In the QAF diagram (Fig. 7a), they plot predominantly into the fields of monzogranite and quartz–rich granite. CIPW-normative calculations show the constitutes of 25–53 vol.% Qz, 8–19 vol.% Or, 13–29 vol.% Ab and 6–16 vol.% An. They are strongly peraluminous with the A/CNK value ranging from 1.15 to 1.48 and contain 1.8–5.0 vol.% corundum (Fig. 7b). Such signatures are similar to those of typical S-type granites, falling into the S-type range in the triangle diagram of $Al_2O_3$–($K_2O + Na_2O$)–(CaO–(FeOt + MgO)) (Fig. 7c).

Our samples give total REE contents from 150 ppm to 361 ppm and δEu values from 0.35 to 0.70. They show steep REE chondrite-normalized patterns with (La/Yb)$n$ = 7.1–14.0 and (Gd/Yb)$n$ = 1.30–2.04 (Fig. 8a). On the primitive mantle- normalized spidergram (Fig. 8b), these samples are characterized by markedly negative Nb-Ta, P, Sr and Ti anomalies, similar to those of the Jingningian (~820 Ma) and Kwangsian (400–460 Ma) peraluminous granites and Precambrian metamorphic volcanosedimentary rocks in the Jiangnan Fold Belt and Cathaysia Block (e.g., Chen and Jahn, 1998; Wan et al., 2007, 2010; Wang et al., 2007a,b, 2012c, Zhang et al., 2013; Zhao et al., 2013). Their initial $^{87}Sr/^{86}Sr$ ratios range from 0.7068 to 0.7233 and $\varepsilon_{Nd}(t)$ values from −3.81 to −9.54 (Fig. 9). The corresponding Nd model ages are in the range of 1.91–2.49 Ga.

## 6. Discussion

### 6.1. Petrogenetic constraints

Our samples show Zr correlating with Rb and Ba, suggesting that their mobility of LILE (e.g., Rb, Sr and Ba) after intrusion of the granitic rocks does not seriously change their contents. Their ratios can be used to constrain the source nature. These samples are strongly peraluminous and K-rich, with the majority having $K_2O/Na_2O > 1$. They have low $SiO_2$, low $Al_2O_3/TiO_2$ and Rb/Sr ratios as well as high $CaO/Na_2O$ ratios (>0.6) relative to the partial melting product of typical meta-pelitic sources, such as leucogranite in Himalaya Orogen (Harris and Inger, 1992; Altherr et al., 2000). In contrast, they are similar to the peraluminous granites in the Lachlan Fold Belt, which were probably derived from meta-greywacke source. Their $\varepsilon$Nd($t$) and $\varepsilon$Hf($t$) values fall into the fields of the global lower crust and global sedimentary rocks (Fig. 9b). In the $Al_2O_3/(MgO + FeOt)$ vs $CaO/(MgO + FeOt)$ diagram (Fig. 10a), these samples plot into the jointed field of the meta-greywacke and metaigneous sources. In the plot of Rb/Sr and Rb/Ba, they fall into the field of the plagioclase-rich and clay-poor crustal source (Fig. 10b). High FeOt, MgO and $TiO_2$ contents, and low $Al_2O_3/(MgO + FeOt)$ and Rb/Sr ratios suggest the involvement of the metaigneous component in the source (Table 4, e.g., Chappell and White, 1992; Sylvester, 1998; Altherr et al., 2000; Anthony, 2005; Wang et al., 2007a,b, 2011a,b).

**Table 3**
Summary of lithology, sampling locations, zircon U–Pb dating and Lu–Hf isotopic results of the representative samples from Cathaysia.

| Sample | Lithology | Sampling location | Inherited zircon age | Crystallization age | $\varepsilon_{Hf}(t)$ | $T_{DM}$ model age |
|---|---|---|---|---|---|---|
| 09WG-44A | Granitic gneiss previously mapped as Mayuan Group | North of Masha, Shaowu, SW Fujian E117°49.911′, N27°24.138′ | | 909 ± 10 Ma, $n$ = 20, MSWD = 0.6 | −5.2 to +1.3 with peak of −2.3 | 1.43–1.67 Ga with peak of 1.56 Ga |
| 09WG-44B | Granitic gneiss previously mapped as Mayuan Group | North of Masha, Shaowu, SW Fujian E117°49.911′, N27°24.138′ | | 916 ± 6 Ma, $n$ = 20, MSWD = 1.0 | −5.8 to +0.6 with peak of −2.2 | 1.35–1.69 Ga with peak of 1.57 Ga |
| 12WY-116C | Granitic gneiss previously mapped as Xuwu Group | Dawei village, Xunwu, SE Jiangxi E 115°19.438′, N 24°57.838′ | 1435 Ma, 1450 Ma, 1472 Ma, 1407 Ma, 1612 Ma, 1700 Ma, 1876 Ma, 2154 Ma, 2492 Ma 2513 Ma, 2653 Ma, 2642 Ma, | 982 ± 27 Ma, $n$ = 8, MSWD = 0.5 | −9.6 to +0.8 with peaks of −2.5 and −8.6 | 1.51–1.89 Ga with peaks of 1.57 Ga and 1.85 Ga |
| 12WY-118A | Granitoid gneiss previously mapped as Xuwu Group | North Longtang, Dingnan, SE Jiangxi E 115°11.360′, N 24°51.920′ | 1265 Ma, 1306 Ma, 1972 Ma, 2074 Ma | 963 ± 11 Ma, $n$ = 17, MSWD = 0.2 | −5.8 to +0.6 with peaks of −2.1 and −7.0 | 1.35–1.69 Ga with peaks of 1.57 Ga and 1.72 Ga |
| 12YK-58C | Granitoid gneiss mapped as Yunkai Group | Shuanglong, Luoding, SW Guangdong E 111°20.082′, N 22°43.093′ | 2028 ± 48 Ma | Upper intercept age of 926 ± 28 Ma | −5.5 to −7.3 with peak of −6.8 | 1.68–1.75 Ga with peak of 1.72 Ga |
| 09YK-6A | Metagranite previously mapped as Yunkai Group | Huaixiang, Xinyi, SW Guangdong E 111°03.286′, N 22°25.818′ | 1068 Ma, 1840 Ma, 1856 Ma, 1856 Ma, 2431 Ma, 2541 Ma, 2573 Ma | 954 ± 14 Ma, $n$ = 7, MSWD = 1.0 | | |

Our samples exhibit similar REE and incompatible elemental pattern and variation of major oxides with the Kwangsian granitic rocks in South China (Fig. 8a and b), which are commonly believed to originate from a Proterozoic metapelitic and meta-igneous source with little addition of newly mantle-derived components (e.g., Wang et al., 2007a,b, 2011a,b; Zhang et al., 2012a). Their $\varepsilon_{Nd}(t)$ values and Nd model ages are also identical to those of the Kwangsian granite in South China when age is back-calculated to 920 Ma (Fig. 11a and b). Such geochemical signatures are also similar to the metamorphic basement in the Wuyi-Yunkai Domains of the Cathaysia consisting of mainly the meta-sedimentary rocks with proportional meta-igneous rocks (e.g., Yu et al., 2005, 2007). The diverse components of the Cathaysia basement provide an ideal source for our earliest Neoproterozoic granite. In the plots of Zr/Nb and Zr/Hf and Nb/La (Fig. 11c and d), they fall into the fields of the Kwangsian granites and show a linear correlation. In addition, our zircon grains with the earliest Neoproterozoic age share the $\varepsilon$Hf($t$) values of −9.64∼+2.78 with the peak values at ca. −2.5 and ca. −7.5, respectively (Table 3 and Fig. 9b). The corresponding Hf model ages range from 1.35 Ga to 2.00 Ga with the peaks of ∼1.57 Ga and ∼1.75 Ga, respectively (Table 3). These observations all suggest a binary mixing of the metapelitic and metaigneous components in the source. The metaigneous component is characterized by low $SiO_2$ and Rb/Sr but high FeO + MgO + $TiO_2$, $\varepsilon$Nd($t$) and $\varepsilon$Hf($t$) values, along with younger Nd and Hf model ages (Fig. 11a–d).

### 6.2. Tectonic implications

Our zircon U–Pb geochronological results for the Masha (NW Fujian) granitic gneiss (09WG-44A and 09WG-44B) yield the weighted mean age of 913 ± 5 Ma ($n$ = 38, MSWD = 0.5). Two gneissoid samples (12WY-116C and 09WG-118A) from Dawei and Longtang (SE Jiangxi) have zircon U–Pb age of 982 ± 27 Ma and

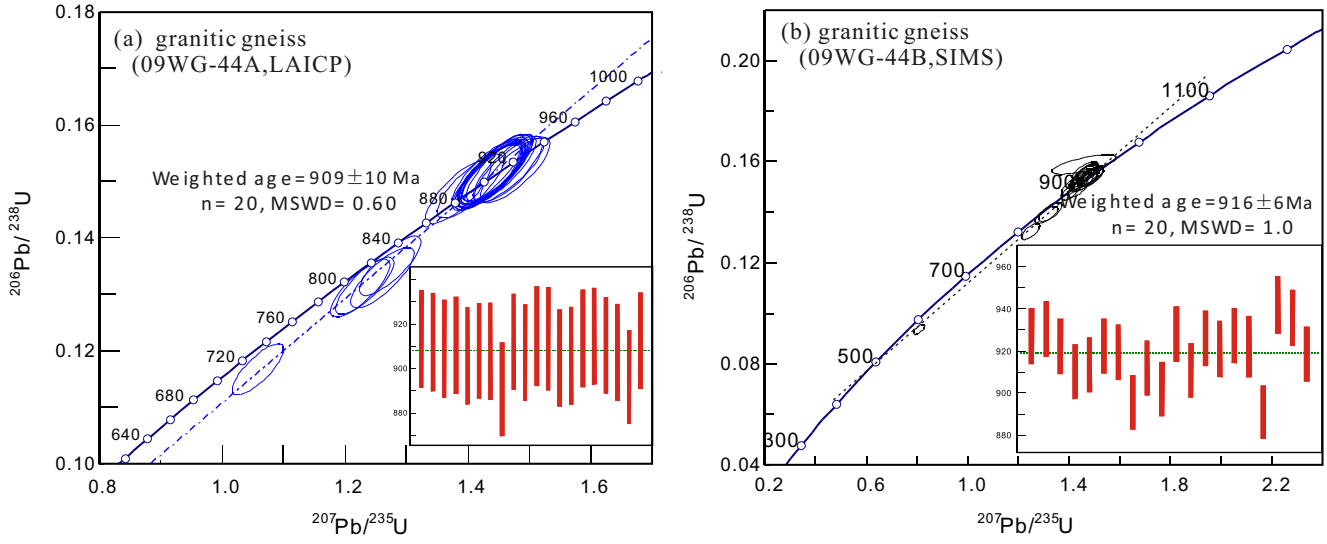


**Fig. 4.** Concordia diagrams of zircon U–Pb data for the granitic gneisses from Masha (Jianyang), the Wuyi Domain, (a) 09WG-44A, (b) 09WG-44B. The locations for these samples are shown in Fig. 1.

**Table 4**
Major oxides, elemental and Sr–Nd isotopic analytical results for the early Neoproterozoic granitic rocks in the Cathaysia Block.

| Sample | 09WG-44A | 09WG-44B | 12WG-44D1 | 12WG-44D2 | 09WG-48A | 09WG-60A | 09WG-60G | 09WG-60H | 09WG-60I | 12WY-116C | 12WY-118A | Hezi* | 12YK-58C | 09YK-6A | 09YK-6B | 09YK-6E | 09YK-6G | 09YK-14B |
|---|---|---|---|---|---|---|---|---|---|---|---|---|---|---|---|---|---|---|
| $SiO_2$ | 66.53 | 65.07 | 67.48 | 67.94 | 69.39 | 67.58 | 66.17 | 67.42 | 70.58 | 71.61 | 66.17 | 66.32 | 64.45 | 72.61 | 73.80 | 75.77 | 73.02 | 70.67 |
| $TiO_2$ | 0.88 | 0.89 | 0.87 | 0.75 | 0.87 | 0.75 | 0.73 | 0.73 | 0.72 | 0.43 | 0.73 | 0.60 | 0.86 | 0.65 | 0.69 | 0.66 | 0.62 | 0.56 |
| $Al_2O_3$ | 14.33 | 14.94 | 14.38 | 14.91 | 12.34 | 13.71 | 13.82 | 13.83 | 11.82 | 13.25 | 14.86 | 15.03 | 15.77 | 12.19 | 11.92 | 11.08 | 11.92 | 14.24 |
| FeOt | 5.93 | 5.68 | 5.84 | 4.77 | 6.08 | 6.41 | 6.10 | 5.94 | 5.42 | 4.74 | 6.08 | 4.55 | 5.01 | 5.32 | 4.77 | 4.17 | 5.06 | 4.60 |
| MgO | 1.59 | 1.65 | 1.53 | 1.31 | 2.67 | 2.70 | 2.67 | 2.59 | 2.70 | 1.54 | 1.54 | 0.88 | 2.83 | 1.81 | 1.65 | 1.53 | 1.91 | 1.77 |
| CaO | 2.25 | 1.96 | 2.20 | 1.95 | 2.05 | 1.65 | 3.14 | 2.59 | 2.40 | 1.60 | 3.12 | 2.11 | 3.33 | 1.28 | 1.27 | 0.87 | 1.33 | 1.53 |
| $K_2O$ | 3.75 | 4.76 | 3.63 | 4.61 | 1.33 | 2.72 | 2.31 | 2.18 | 2.70 | 1.81 | 4.08 | 4.63 | 3.98 | 2.42 | 2.44 | 2.40 | 2.10 | 2.09 |
| $Na_2O$ | 2.24 | 2.26 | 2.27 | 2.14 | 2.55 | 1.78 | 2.55 | 2.82 | 1.48 | 2.54 | 1.92 | 2.18 | 1.86 | 2.00 | 1.84 | 1.51 | 2.17 | 2.83 |
| MnO | 0.06 | 0.05 | 0.06 | 0.04 | 0.07 | 0.07 | 0.06 | 0.06 | 0.07 | 0.08 | 0.05 | 0.06 | 0.08 | 0.06 | 0.05 | 0.04 | 0.05 | 0.04 |
| $P_2O_5$ | 0.05 | 0.13 | 0.05 | 0.16 | 0.09 | 0.09 | 0.12 | 0.12 | 0.12 | 0.06 | 0.17 | 0.24 | 0.11 | 0.15 | 0.15 | 0.15 | 0.13 | 0.12 |
| LOI | 1.77 | 1.98 | 1.58 | 1.31 | 1.95 | 1.94 | 1.77 | 1.19 | 1.37 | 1.87 | 1.14 | | 1.12 | 1.30 | 1.28 | 1.29 | 1.54 | 1.38 |
| Total | 99.38 | 99.38 | 99.88 | 99.88 | 99.38 | 99.42 | 99.46 | 99.47 | 99.38 | 99.51 | 99.87 | 96.60 | 99.40 | 99.79 | 99.85 | 99.48 | 99.86 | 99.84 |
| A/NK | 1.85 | 1.68 | 1.87 | 1.75 | 2.19 | 2.33 | 2.06 | 1.97 | 2.20 | 2.16 | 1.96 | 1.75 | 1.90 | 2.06 | 2.10 | 2.18 | 2.04 | 2.06 |
| A/CNK | 1.35 | 1.26 | 1.37 | 1.37 | 1.18 | 1.27 | 1.19 | 1.18 | 1.15 | 1.48 | 1.43 | 1.47 | 1.19 | 1.32 | 1.37 | 1.41 | 1.28 | 1.40 |
| Cr | | | | | | 76.4 | 73.2 | 73.0 | 68.8 | 54.4 | 64.7 | | 42.8 | 69.0 | 62.0 | 38.5 | 68.9 | 69.6 |
| Co | | | | | | 17.4 | 15.7 | 15.6 | 11.4 | 11.6 | 13.1 | | 12.7 | 11.8 | 9.1 | 7.9 | 11.2 | 9.6 |
| Ni | | | | | | 36.1 | 34.5 | 33.6 | 29.8 | 22.5 | 46.2 | | 27.6 | 27.3 | 23.4 | 18.9 | 26.3 | 25.6 |
| Ga | 22.00 | 21.49 | 20.56 | 21.12 | 17.42 | 17.97 | 17.15 | 17.62 | 14.50 | 22.20 | 12.58 | | 21.37 | 16.47 | 15.08 | 13.26 | 15.59 | 18.37 |
| Rb | 156 | 178 | 81 | 84 | 83 | 84 | 97 | 86 | 120 | 138 | 79 | | 87 | 114 | 105 | 86 | 104 | 113 |
| Sr | 122 | 126 | 321 | 333 | 245 | 112 | 290 | 158 | 119 | 125 | 84 | | 299 | 108 | 108 | 84 | 121 | 125 |
| Y | 52.62 | 44.86 | 27.61 | 27.96 | 24.42 | 24.87 | 27.42 | 27.25 | 22.53 | 33.46 | 11.43 | | 42.60 | 27.20 | 26.35 | 21.53 | 26.57 | 32.15 |
| Zr | 311 | 305 | 167 | 171 | 225 | 210 | 190 | 221 | 230 | 198 | 197 | | 282 | 274 | 300 | 209 | 244 | 288 |
| Nb | 15.18 | 14.01 | 10.59 | 10.94 | 16.78 | 15.05 | 14.14 | 14.92 | 13.50 | 20.80 | 8.96 | | 14.32 | 18.06 | 18.25 | 12.81 | 12.38 | 12.97 |
| Ba | 733 | 974 | 463 | 477 | 475 | 721 | 459 | 573 | 470 | 96 | 558 | | 655 | 528 | 624 | 661 | 572 | 455 |
| La | 72.82 | 66.60 | 28.58 | 28.69 | 45.91 | 45.74 | 44.64 | 49.58 | 36.31 | 41.11 | 33.61 | | 49.74 | 45.64 | 46.87 | 53.37 | 42.42 | 39.82 |
| Ce | 146.7 | 136.3 | 58.49 | 58.36 | 95.39 | 87.50 | 89.48 | 94.31 | 72.91 | 81.57 | 66.23 | | 105.3 | 93.20 | 98.49 | 102.5 | 83.35 | 77.76 |
| Pr | 18.56 | 16.93 | 7.17 | 7.22 | 10.88 | 10.43 | 10.39 | 11.25 | 8.79 | 9.34 | 7.75 | | 13.56 | 11.13 | 11.80 | 12.25 | 10.01 | 9.52 |
| Nd | 68.98 | 63.42 | 28.70 | 28.58 | 39.56 | 37.55 | 38.36 | 41.16 | 32.70 | 33.37 | 28.33 | | 54.01 | 39.73 | 41.45 | 43.62 | 35.64 | 34.53 |
| Sm | 13.64 | 12.03 | 5.89 | 5.86 | 7.20 | 6.61 | 7.01 | 7.49 | 6.14 | 6.89 | 5.58 | | 10.75 | 7.06 | 7.36 | 7.67 | 6.55 | 6.80 |
| Eu | 1.49 | 1.58 | 1.51 | 1.51 | 1.31 | 1.30 | 1.40 | 1.43 | 1.13 | 0.65 | 1.04 | | 1.70 | 1.35 | 1.44 | 1.17 | 1.31 | 1.44 |
| Gd | 11.83 | 10.73 | 5.79 | 5.75 | 5.98 | 5.66 | 6.04 | 6.31 | 5.21 | 6.27 | 4.52 | | 9.40 | 6.22 | 6.33 | 6.51 | 6.22 | 6.32 |
| Tb | 1.88 | 1.68 | 0.94 | 0.96 | 0.92 | 0.87 | 0.89 | 0.96 | 0.80 | 1.06 | 0.62 | | 1.55 | 0.90 | 0.91 | 0.87 | 0.87 | 0.97 |
| Dy | 10.05 | 9.03 | 5.63 | 5.54 | 5.00 | 5.01 | 5.08 | 5.48 | 4.56 | 6.20 | 2.92 | | 8.50 | 5.01 | 4.85 | 4.33 | 4.80 | 5.53 |
| Ho | 2.14 | 1.79 | 1.14 | 1.16 | 0.96 | 1.03 | 1.05 | 1.08 | 0.88 | 1.24 | 0.49 | | 1.73 | 0.97 | 0.96 | 0.76 | 0.93 | 1.10 |
| Er | 5.84 | 4.94 | 3.16 | 3.18 | 2.69 | 2.88 | 2.90 | 2.98 | 2.32 | 3.22 | 1.14 | | 4.74 | 2.73 | 2.62 | 1.99 | 2.63 | 3.37 |
| Tm | 0.85 | 0.68 | 0.45 | 0.45 | 0.38 | 0.43 | 0.44 | 0.44 | 0.34 | 0.46 | 0.15 | | 0.71 | 0.40 | 0.40 | 0.29 | 0.38 | 0.58 |
| Yb | 5.13 | 4.30 | 2.89 | 2.91 | 2.43 | 2.75 | 2.77 | 2.82 | 2.17 | 2.78 | 0.95 | | 4.84 | 2.69 | 2.57 | 1.79 | 2.62 | 4.42 |
| Lu | 0.73 | 0.64 | 0.44 | 0.45 | 0.37 | 0.43 | 0.43 | 0.43 | 0.34 | 0.41 | 0.14 | | 0.73 | 0.40 | 0.39 | 0.27 | 0.38 | 0.71 |
| Hf | 9.18 | 8.45 | 4.80 | 4.81 | 6.40 | 6.07 | 5.48 | 6.12 | 6.68 | 5.62 | 5.70 | | 7.83 | 7.49 | 8.17 | 2.44 | 6.48 | 7.81 |
| Ta | 0.84 | 0.71 | 0.75 | 0.76 | 0.70 | 0.92 | 0.88 | 0.93 | 1.06 | 1.93 | 0.89 | | 0.90 | 1.17 | 1.19 | 1.18 | 1.09 | 1.49 |
| Pb | 27.83 | 29.70 | 10.24 | 10.89 | 19.88 | 15.03 | 24.17 | 22.27 | 14.21 | 16.33 | 20.21 | | 10.47 | 33.10 | 24.91 | 22.02 | 24.19 | 19.72 |
| Th | 32.41 | 26.15 | 8.75 | 8.59 | 21.09 | 18.76 | 19.06 | 21.35 | 15.22 | 22.83 | 15.31 | | 14.20 | 19.34 | 21.05 | 23.09 | 19.09 | 17.17 |
| U | 3.61 | 2.60 | 1.74 | 1.70 | 1.36 | 2.01 | 1.97 | 2.65 | 2.36 | 9.26 | 2.21 | | 2.51 | 3.59 | 3.83 | 3.69 | 3.46 | 4.20 |
| $T$(°C) | 862 | 854 | 808 | 817 | 789 | 791 | 778 | 795 | 788 | 828 | 824 | | 817 | 843 | 860 | 771 | 827 | 858 |
| $^{87}Rb/^{86}Sr$ | 3.69 | 4.09 | 0.73 | 0.73 | 0.99 | | | | | 3.20 | 2.72 | | 0.85 | 3.07 | 2.83 | | | |
| $^{87}Sr/^{86}Sr$ | 0.771810 | 0.769135 | 0.721042 | 0.720915 | 0.724136 | | | | | 0.761410 | 0.745140 | | 0.717902 | 0.753147 | 0.751831 | | | |
| 2 σ | 6 | 6 | 5 | 5 | 6 | | | | | 13 | 12 | | 6 | 12 | 10 | | | |
| $(^{87}Sr/^{86}Sr)_i$ | 0.72331 | 0.71533 | 0.71148 | 0.71133 | 0.71114 | | | | | 0.716560 | 0.707022 | | 0.70679 | 0.71184 | 0.71459 | | | |
| $^{147}Sm/^{144}Nd$ | 0.120 | 0.115 | 0.124 | 0.124 | 0.110 | | | | | 0.125 | 0.119 | | 0.120 | 0.107 | 0.107 | | | |
| $^{143}Nd/^{144}Nd$ | 0.511935 | 0.511913 | 0.511992 | 0.511999 | 0.511628 | | | | | 0.511704 | 0.511896 | | 0.511982 | 0.511630 | 0.511666 | | | |
| 2 σ | 3 | 4 | 3 | 5 | 3 | | | | | 7 | 6 | | 3 | 7 | 6 | | | |
| εNd ($t$) | −4.64 | −4.51 | −4.08 | −3.92 | −9.54 | | | | | −9.23 | −4.77 | | −3.81 | −8.95 | −8.47 | | | |
| $T_{DM}$(Ga) | 1.97 | 1.91 | 1.98 | 1.96 | 2.25 | | | | | 2.49 | 2.03 | | 1.91 | 2.19 | 2.13 | | | |

$T$(°C): zircon saturation temperature. εNd ($t$): εNd values when time back-calculated to 950 Ma. $T_{DM}$(Ga): Nd model age.
* Sample cited from Liu et al. (2001).

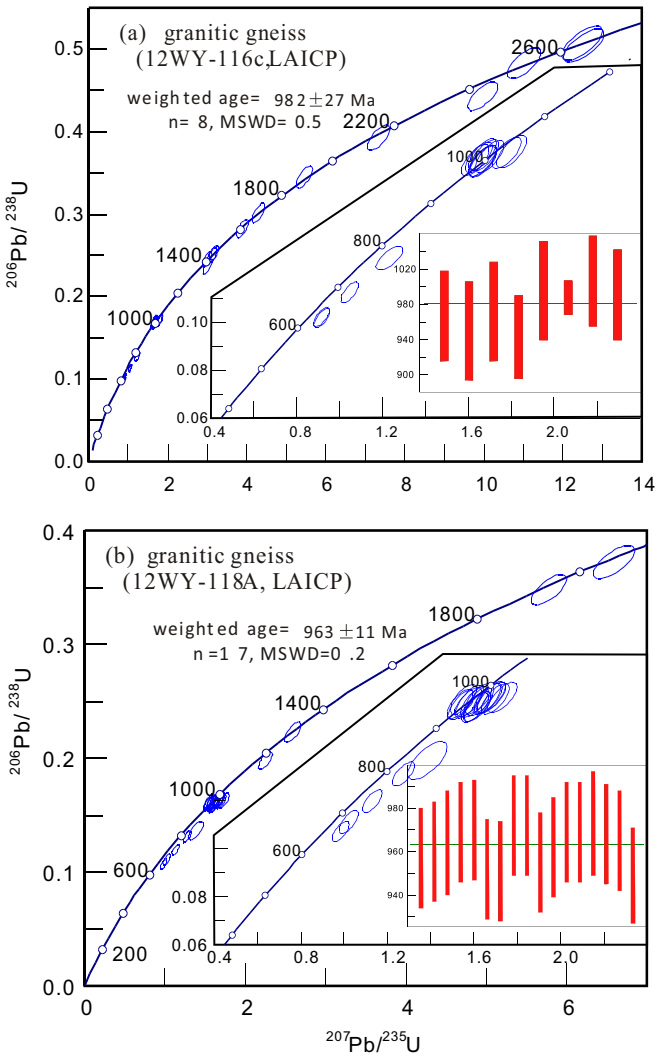


**Fig. 5.** Concordia diagrams of zircon U–Pb data for the granitic gneisses from Dawei (Xunwu) and Longtang (Dingnan), SE Jiangxi, the Nanling Domain. (a) 12WY-116c from Dawei (Xunwu), (b) 12WY-118A from Longtang (Dingnan). Sample locations are shown in Fig. 1.

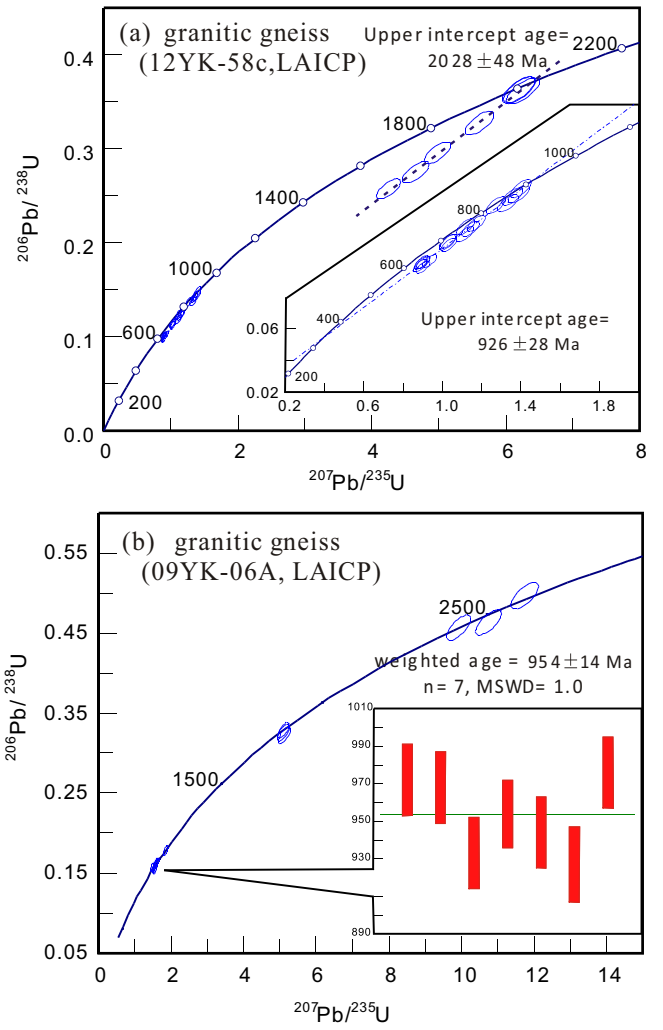


**Fig. 6.** Concordia diagrams of zircon U–Pb data for the granitic gneisses from Shuanglong (Luoding) and Huaixiang (Xinyi), SW Guangdong, the Yunkai Domain. (a) 12YK-58c from Shuanglong (Luoding), (b) 09YK-06A from Huaixiang (Xinyi). Sample locations are shown in Fig. 1.

963 ± 11 Ma, respectively. The granitic gneisses from SW Guangdong give the zircon U–Pb ages of 926 ± 28 Ma (12YK-58C) and 954 ± 14 Ma (09YK-6A), respectively. These ages can be interpreted as the crystallization time of these granitic rocks. Shu et al. (2008, 2011) and Liu et al. (2001) reported the SHRIMP zircon U–Pb age of 972 ± 8 Ma and the Pb–Pb age of 996 ± 29 Ma for the rhyolite and granodiorite from Jingnan (NE Guangdong) and Hezi (SE Jiangxi), respectively. The dacite-porphyry in the Yunkai complex has the zircon evaporate age of ~1000 Ma (Zhang et al., 1997). In addition, the late Neoproterozoic and Paleozoic sedimentary rocks in the Jianyang, Zengcheng, Nanxiong and Xinyi areas of the Cathaysia Block contain abundant detritus zircons with the U–Pb ages of ~0.92–1.0 Ga with the peak age of ~940 Ma (e.g., Yu et al., 2007; Wang et al., 2007c, 2008c, 2010a,b; Wan et al., 2007, 2010; Li et al., 2011). The inherited grains with the U–Pb age of ~0.90–1.0 Ga were also observed in the Kwangsian gneissic and massive granites in the Cathaysia Block (e.g., Ding et al., 2005; Wang et al., 2011a,b; Zhang et al., 2012b). These data evidenced the development of the earliest Neoproterozoic (~913–982 Ma) magmatism along the Wuyi-Yunkai domain in the Cathaysia interior (e.g., Shu et al., 2008, 2011).

The generation of S-type granites is usually related to continental-collisional and intraplate orogenic regimes or the closure of back-arc basins (e.g., Pearce, 1996; Sylvester, 1998; Brown, 2001; Atherton and Ghani, 2002; Clemens, 2003; Healy et al., 2004; Wang et al., 2007a,b, 2013a,b). Along the Wuyi-Yunkai domain of the Cathaysia Block, small amounts of the earliest Neoproterozoic (~969–997 Ma) mafic and ultramafic rocks were recently identified (e.g., Zhang et al., 2012a; Wang et al., 2013a,b). These metabasic rocks occur as lens, pods and fragment in the high-grade metamorphic basement and geochemically signify the development of a ~970–1000 Ma arc-back-arc system (e.g., Zhang et al., 2012a; Wang et al., 2013a,b). Shu et al. (2008, 2011) and Zhang et al. (1997) also proposed that the 972 Ma rhyolitic rocks in Nanling (NE Guangdong) and synchronous dacite porphyry in SW Guangdong (Yunkai) formed in a volcanic arc setting. In the Shuangxiwu-Zhangshudun area, there preserved arc-type volcanic series and dismembered ophiolitic association that were dated at ~905–980 Ma. These data indicate an earliest Neoproterozoic (~970 Ma) active continental margin rather than intraplate tectonic regime along the Wuyi-Yunkai belt of the Cathaysia Block. Our samples have zircon saturation temperature of 790–862 °C with the peak temperature at ~820 °C (Table 4). Their $Al_2O_3/TiO_2$ ratios range from 16.3 to

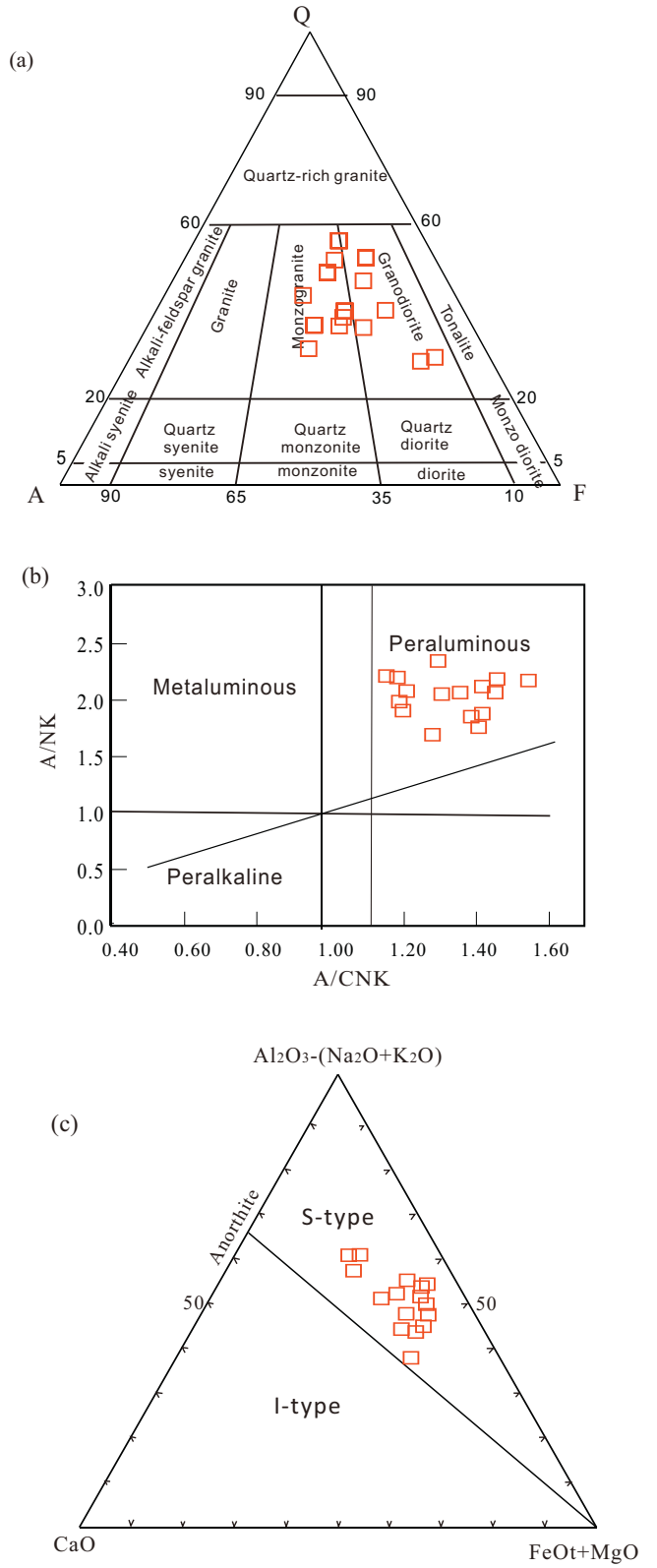


**Fig. 7.** (a) QAF diagram, (b) A/CNK vs A/NK (a), and (c) $CaO–FeOt+MgO–Al_2O_3–(Na_2O+K_2O)$ for the early Neoproterozoic granitic gneisses from the Cathaysia interior. Symbols in (b and c) are the same as those in Fig. 5a.

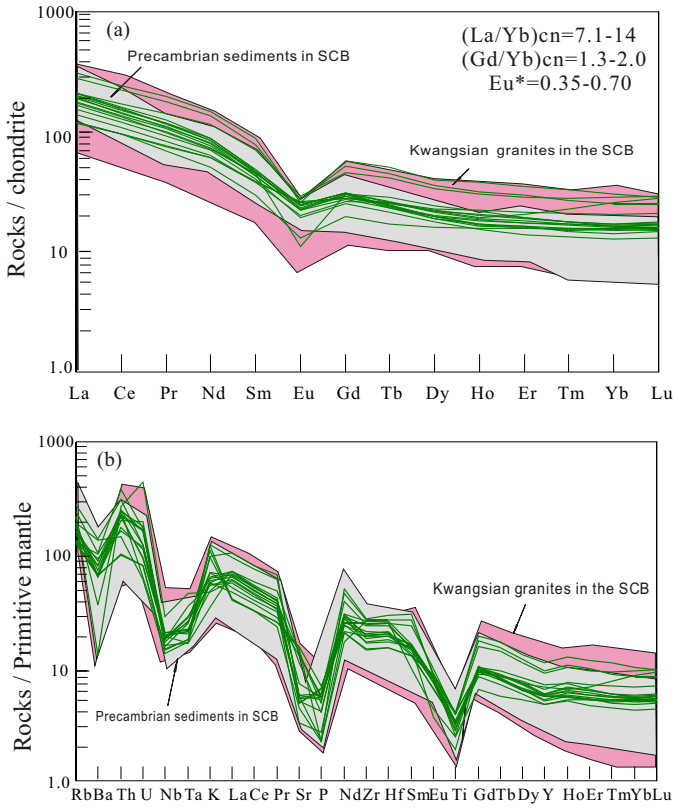


**Fig. 8.** (a) Chondrite-normalized rare earth element and (b) primitive mantle-normalized incompatible elemental patterns for the early Neoproterozoic granitic gneisses within the Cathaysia Block. Normalized values for chondrite and primitive mantle are from Taylor and McLennan (1985) and Sun and McDonough (1989), respectively. Also shown are the patterns for Kwangsian granitic rocks (e.g., Wang et al., 2007a,b; Wan et al., 2007; Zeng et al., 2008; Wang et al., 2012c; Zhang et al., 2013) and Precambrian sedimentary rocks in the SCB (Wan et al., 2007, 2010; Wang et al., 2012c).

30.8 (Table 4), further indicating the high-temperature petrogenesis of the granites (e.g., Sylvester, 1998). It is general that the high-temperature granites are preponderantly generated in rifting- or subduction-related regimes (e.g., Sylvester, 1998). However, the granitic magma in a rift setting usually shows I- and A-type geochemical affinity and has a significant input of juvenile materials. However, our samples are characterized by S-type granites and were derived from the mixing source of metapelitic and metaigneous components with little input from juvenile components. This dismisses any possibility of these granites generating in a rifting setting. On the discrimination diagrams of Rb-Y + Nb and Nb-Y (e.g., Harris et al., 1986; Pearce et al., 1984; Pearce, 1996), these samples plot into the field of volcanic arc granites or overlapping fields of the arc- and syncollisional granites (Fig. 12a and b). Therefore, the synthesis of these data indicates that the S-type granites might be petrogenetically linked to the closure of a back-arc tectonic setting. In fact, along the Phanerozoic circum-Pacific orogenic belts, the majority of "postcollisional" S-type granites formed in an early arc/back-arc regime, as illustrated by the Lachlan and New England fold belts of the Terra Australis accretionary orogenic system (e.g., Clemens, 2003; Collins and Richards, 2008; Kemp et al., 2009; Cawood et al., 2009, 2011). Wang et al. (2013a,b) also considered that the formation of early Paleozoic S-type granites in Sibumasu of SW Yunnan was geodynamically related to the closure of the back-arc basin in an accretionary continental margin setting.

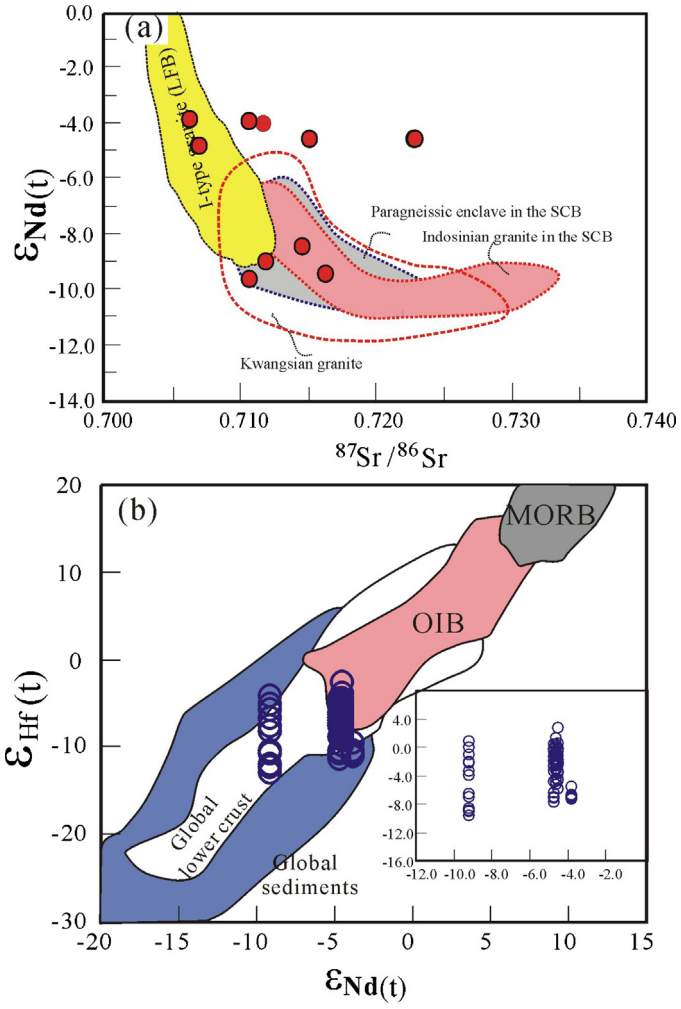


**Fig. 9.** (a) Initial Sr–Nd isotopic composition and (b) $\varepsilon$Nd(t) versus $\varepsilon$Hf(t) of the early Neoproterozoic granitic gneisses in the Cathaysia Block. Also shown in (a) are those for the Ordovician sedimentary rocks, S- and I-type granites from the Lachlan Fold Belt are from Healy et al. (2004). The data for the Indosinian and Kwangsian granitic rocks and paragneiss enclave in the SCB are from Huang and Depaolo (1989), Wan et al. (2007, 2010); Zeng et al. (2008); Wang et al. (2007a,b, 2012c) and Zhang et al. (2013).

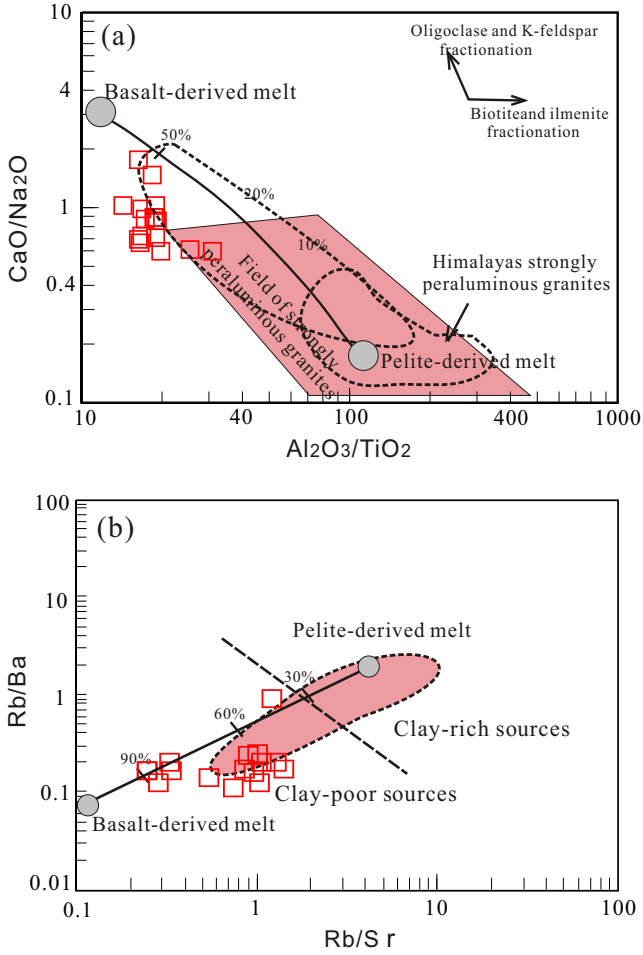


**Fig. 10.** $Al_2O_3/TiO_2$ versus $CaO/Na_2O$ (a) and Rb/Sr versus Rb/Ba (b) for the early Neoproterozoic granitic gneisses in Cathaysia. The mixing curve between the basalt- and pelite-derived melts in (a and b) is from Patiño-Douce and Harris (1998) and Sylvester (1998).

A question remains as to what time for the closure of the back-arc basin? Wang et al. (2013a,b) and Zhang et al. (2012) proposed that the Wuyi-Yunkai arc-back-arc system developed at ~969–997 Ma. Greentree et al. (2006) proposed the earliest Neoproterozoic (~960 Ma) sedimentary succession deposited in a foreland basin, indicative of the back-arc basin being inverted to be a compressive basin. The detrital zircons in the late Neoproterozoic sedimentary rocks commonly show an igneous origin and give U–Pb ages of ~0.90–1.0 Ga (peak age being ~940 Ma) along the Wuyi-Yunkai area (e.g., Yu et al., 2007, 2010; Wan et al., 2007, 2010; Wang et al., 2007c, 2008c, 2010b, 2008b). These data, together with the formation age of 913–926 Ma for Masha and Longtang S-type granitic rocks, indicate that the Wuyi-Yunkai arc-back-arc system might be finally closed at ~920 Ma (e.g., Yu et al., 2010; Zhang et al., 2012a; Wang et al., 2013a and reference therein). During the process, the accumulated sedimentary rocks in the earliest Neoproterozoic back-arc basin were significantly thickened to induce the crustal anatexis for producing the S-type granites. This process is also evidenced by the 1.0 Ga zircon overgrowths in sample 97HN93 from the Baobang Group in the Hainan domain of the Cathaysia Block. The Mamianshan bimodal volcanic rocks and OIB-type mafic rocks at Wuyi formed in a continental rift or intra-plate setting, and were dated at ~890–790 Ma (e.g., Li et al., 2005, 2010b; Shu et al., 2006, 2008, 2011), further constraining the closure time of the Wuyi-Yunkai arc-basin system being closed before 890 Ma.

Numerous data show that the Shuangxiwu arc or back-arc system developed at 970–910 Ma and terminated at around 880–890 Ma (e.g., Li et al., 2005, 2010b), younger than those of the Wuyi-Yunkai arc-back-arc system (e.g., Wang et al., 2013a,b). The back-arc basin or "Huanan ocean" along the Jiangnan orogen developed since ~890 Ma and its final closure occurred at ~830–820 Ma (e.g., Zhao et al., 2011; Wang et al., 2007b, 2011a; Zhou et al., 2009; Ma et al., 2009; Zhang et al., 2012a, 2013; Zhao and Cawood, 2012 and reference therein). This indicates that the previously-defined Cathaysia block might not be a united block but the aggregation of various fragments (e.g., eastern and western Cathaysia) separated by the arc-back-arc systems (e.g., Wuyi- Yunkai, Shuangxiwu and Jiangnan) prior to the early Neoproterozoic period (see Fig. 13a). The Wuyi-Yunkai arc-back-arc system might be the part of the Neoproterozoic arc-basin system of the SCB.

A series of events can be inferred based on available data. A long-lived early Neoproterozoic (950–735 Ma) oceanic subduction and related arc-basin system (e.g., Panxi-Hannan and Ailaoshan) developed along the western and northern, even southern, margins of the Yangtze Block (e.g., Zhao et al., 2011, 2013; Zhao and Cawood, 2012; Cai et al., 2014 and references therein). At ~1000 Ma the subduction of oceanic lithosphere beneath the western/northern Yangtze Block most likely led to the development of various

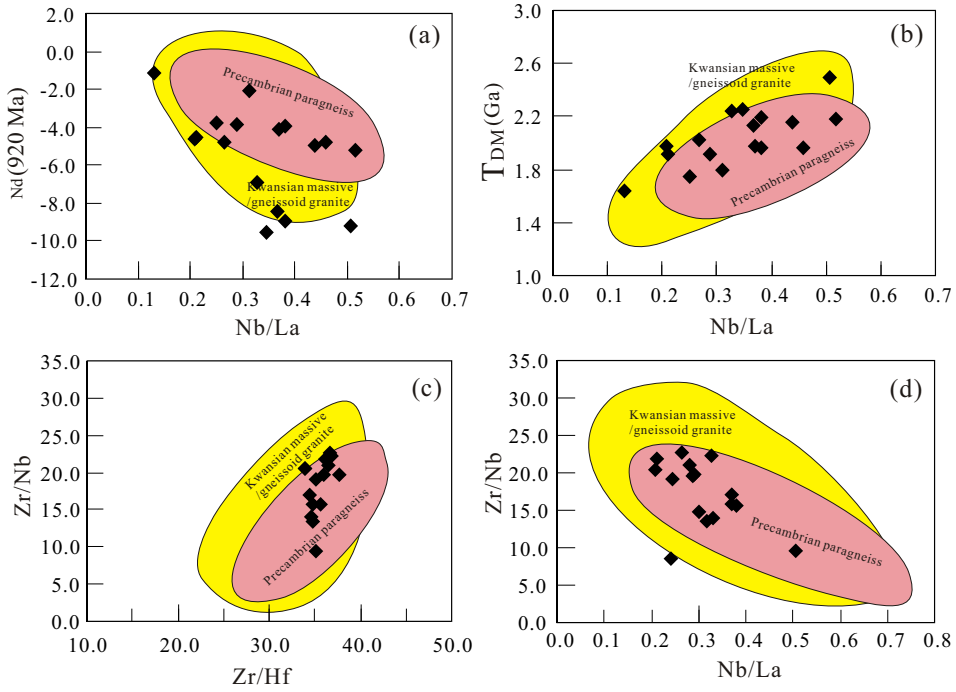


**Fig. 11.** (a and b) Nb/La versus $\varepsilon$Nd (920 Ma) and $T_{DM}$ (Ga), (c and d) Zr/Nb versus Zr/Hf and Nb/La for the early Neoproterozoic granitic gneisses in the Cathaysia Block. Also shown is the range of the Kwangsian massive/gneissic granitic rocks and Precambrian paragneisses in the SCB (e.g., Huang and Depaolo, 1989; Wan et al., 2007, 2010; Zeng et al., 2008; Wang et al., 2007a,b, 2012c, 2013a,b; Zhang et al., 2013).

arc-back-arc systems in the SCB, including Wuyi-Yunkai (Fig. 13b). At ~920–970 Ma (Fig. 13c), the Wuyi-Yunkai arc-back-arc system was finally closed and led to the formation of the Shuangxiwu back-arc system in response to the assembly of Rodinia. The closure of the Shuangxiwu arc-back-arc system and associated orogenesis further resulted in the accretion of the East Cathaysia northward to West Cathaysia till ~890 Ma (Fig. 13d). The continued subduction along the western margin of the Yangtze Block then initiated the development of the Jiangnan arc-back-arc system and the associated magmatism in the eastern SCB (Fig. 5e). At ~800–830 Ma, the closure of the Jiangnan BABB ended the amalgamation of the Yangtze with Cathaysia Blocks and finally formed the united SCB (Fig. 13f).

In summary, the SCB is finally formed by the amalgamation of the various fragments due to the northwesterly episodic closure of a series of arc-back arc systems along Wuyi-Yunkai, Shuangxiwu and Jiangnan at ~920 Ma, ~890 Ma and ~820 Ma, respectively (Fig. 13b–f), significantly younger than the global Grenvillian (~1.0–1.3 Ga) orogenic event along Laurentia, Australia and east Antarctica (e.g., Boger et al., 2000; Jayananda et al., 2000). It would be impossible for such a continuing and long-lived amalgamation to develop within the central Rodinia supercontinent. Our data suggest that the SCB was most likely located on the margin of Rodinia (e.g., Zhang et al., 1997; Yang et al., 2004; Cawood et al., 2010; Cawood et al., 2013; Wang et al., 2013a,b). The early Neoproterozoic progressive amalgamation process of the SCB might be part of an exterior accretionary orogen between Western Australia and East Antarctica around the periphery of Rodinia (e.g., Cawood et al., 2013; Cawood et al., 2007, 2010; Wang et al., 2010a,b, 2013a,b).

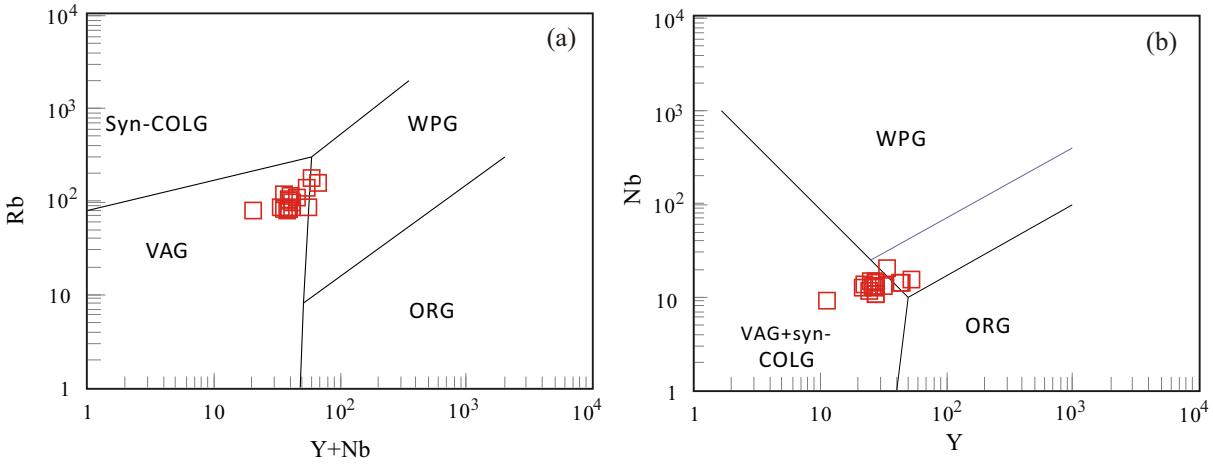


**Fig. 12.** (a) Y + Nb vs Rb and (b) Y vs. Nb for the early Neoproterozoic granitic gneisses in the Cathaysia interior. Syn-COLG, VAG, WPG and ORG note syncollisional granite, volcanic arc granite, within-plate granite and ocean ridge granite, respectively.

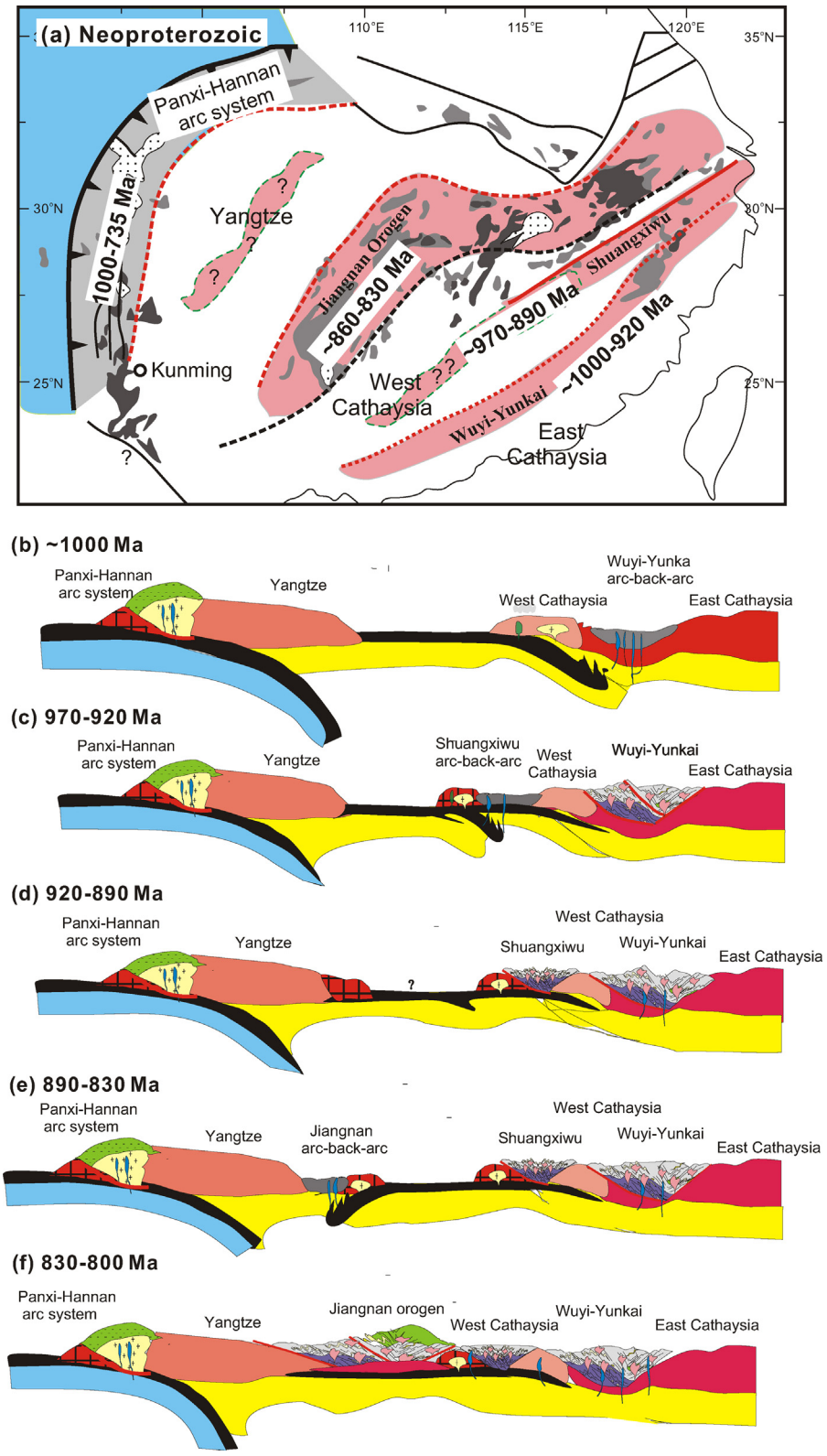


**Fig. 13.** (a) Simplified geological sketch of the South China Block showing the early Neoproterozoic (950–735 Ma) tectonic pattern, and (b–f) Schematic cartoon showing the early Neoproterozoic tectonic evolution of the South China Block. (b) At ~1.0 Ga, the development of the Wuyi-Yunkai arc-back-arc system in response to the subduction of oceanic lithosphere beneath the western/northern Yangtze Block. (c) At ~970–920 Ma, the closure of the Wuyi-Yunkai arc-back-arc system and the formation of the Shuangxiwu back-arc system. (d) At ~920–890 Ma, the accretion of East Cathaysia northward on West Cathaysia due to the closure of the Shuangxiwu arc-back-arc system; (e) the development of the Jiangnan arc-back-arc system and the associated magmatism at ~890–830 Ma in response to the assembly of Rodinia. (f) At ~800–830 Ma, the final amalgamation of the Yangtze with the merged Cathaysia Block along the Jiangnan Orogen. The long-lived subduction along the periphery of Rodinia resulted in the episodic amalgamation of the various fragments of the SCB by the closure of the Wuyi-Yunkai, Shuangxiwu and Jiangnan arc-back arc systems.

## 7. Conclusions

A comprehensive geochemical, zircon U–Pb geochronological and Lu–Hf isotopic study on the granitic gneisses along the Wuyi-Yunkai Domains of the Cathaysia allows us to derive the following conclusions.

(1) Six granitic gneisses from the Wuyi-Yunkai domain yield zircon U–Pb age of 913–982 Ma, indicating the development of the earliest Neoproterozoic magmatism in the Cathaysia interior.
(2) The granitic rocks are characterized by K-rich, strongly peraluminous S-type rocks and originated from the metapelitic coeval with metaigneous source with little addition of juvenile materials.
(3) The S-type granites might be petrogenetically related to the closure of the earliest Neoproterozoic Wuyi-Yunkai back-arc basin at ~980–910 Ma and the SCB most likely located on the margin of Rodinia.

## Acknowledgements

We would like to thank Drs. A-M Zhang and X-P Xia for their help in this field work and the zircon U–Pb analyses. We would like to thank Prof. G-C Zhao and two anonymous reviewers for their critical and constructive reviews on this paper. Dr. Y-H Zhang is thanked for polishing the English. This study benefited from financial supports by National Basic Research Program of China (2014CB440901), Natural Science Foundation of China (41372198), "Closure of Eastern Paleotethys Ocean and Assembly of South China continents" (41190073) that is the 3rd research project of a Major NSFC Program (41190070) and the State Key Laboratory of Ore deposit Geochemistry, CAS (201301).

## References

Altherr, R., Holl, A., Hegner, E., Langer, C., Kreuzer, H., 2000. High-potassium, calc-alkaline plutonism in the European Variscides: northern Vosges (France) and northern Schwarzwald (Germany). Lithos 50, 51–73.
Anthony, E.Y., 2005. Source regions of granites and their links to tectonic environment: examples from the western United States. Lithos 80, 61–74.
Atherton, M.P., Ghani, A.A., 2002. Slab breakoff: a model for Caledonian, late granite syn-collisional magmatism in the orthotectonic (metamorphic) zone of Scotland and Donegal, Ireland. Lithos 62, 65–85.
Boger, S.D., Carson, C.J., Wilson, C.J.L., Fanning, C.M., 2000. Neoproterozoic deformation in the Radok Lake region of the northern Prince Charles Mountains, east Antarctica: evidence for a single protracted orogenic event. Precamb. Res. 104, 1–24.
Brown, M., 2001. Crustal melting and granite magmatism: key issues. Phys. Chem. Earth (A) 26, 201–212.
Cai, Y.F., Wang, Y.J., Cawood, P.A., Fan, W.M., Liu, H.C., Xing, X.W., Zhang, Y.Z., 2014. Neoproterozoic subduction along the Ailaoshan zone, South China: geochronological and geochemical evidence from amphibolite. Precamb. Res. 245, 13–28.
Cawood, P.A., Kröner, A., Collins, W.J., Kusky, T.M., Mooney, W.D., Windley, B.F., 2009. Accretionary orogens through Earth history. In: Cawood, P.A., Kröner, A. (Eds.), Earth Accretionary Systems in Space and Time, vol. 318. Geological Society of London Special Publication, pp. 1–36.
Cawood, P.A., Leitch, E.C., Merle, R.E., Nemchin, A.A., 2011. Orogenesis without collision: stabilizing the Terra Australis accretionary orogen, eastern Australia. Geol. Soc. Am. Bull. 123 (11–12), 2240–2255.
Cawood, P.A., Nemchin, A.A., Strachan, R.A., Prave, T., Krabbendam, M., 2007. Sedimentary basin and detrital zircon record along East Laurentia and Baltica during assembly and breakup of Rodinia. J. Geol. Soc. 164, 251–275.
Cawood, P.A., Strachan, R., Cutts, K., Kinny, P.D., Hand, M., Pisarevsky, S., 2010. Neoproterozoic orogeny along the margin of Rodinia: Valhalla orogen, North Atlantic. Geology 38, 99–102.
Cawood, P.A., Wang, Y.J., Xu, Y.J., Zhao, G.C., 2013. Locating south China in Rodinia and Gondwana: a fragment of greater India lithosphere? Geology, http://dx.doi.org/10.1130/G34395.1.
Chappell, B.W., White, A.J.R., 1992. I- and S-type granites in the Lachlan fold belt. Trans. R. Soc. Edinburgh Earth Sci. 83, 1–26.
Charvet, J., Shu, L.S., Faure, M., Choulet, F., Wang, B., Lu, H.F., Breton, N.L., 2010. Structural development of the Lower Paleozoic belt of South China: genesis of an intracontinental orogen. J. Asian Earth Sci. 39, 309–330.
Charvet, J., Shu, L.S., Shi, Y.S., Guo, L.Z., Faure, M., 1996. The building of South China, collision of Yangzi and Cathaysia blocks, problems and tentative answers. J. Southeast Asian Earth Sci. 13 (3–5), 223–235.
Clemens, J.D., 2003. S-type granitic magmas-petrogenetic issues, models and evidence. Earth Sci. Rev. 61, 1–18.
Collins, W.J., Richards, S.W., 2008. Geodynamic significance of S-type granites in circum-Pacific orogens. Geology 36, 559–562.
Ding, X., Zhou, X.M., Sun, T., 2005. The episodic growth of the continental crustal basement in South China: single zircon LA-ICPMS U–Pb dating of Guzhai granodiorite in Guangdong. Geol. Rev. 51 (4), 383–392.
Fujian BGMR (Bureau of Geology and Mineral Resources of Fujian Province), (in Chinese with English abstract) 1985. Regional Geology of the Fujian Province. Geological Publishing House, Beijing, pp. 1–610.
Gao, J., Klemd, R., Long, L.L., Xiong, X.M., Qian, Q., 2009. Adakitic signature formed by fractional ophiolitic mélange belt, South China. Lithos 110, 277–293.
Gao, S., Lin, W.L., Qiu, Y.M., 1999. Contrasting geochemical and Sm-Nd isotopic compositions of Archaean metasediments from the Kongling high-grade terrain of the Yangtze craton: evidence for cratonic evolution and redistribution of REE during crustal anatexis. Geochim. Cosmochim. Acta 13/14, 2071–2088.
Gao, S., Yang, J., Zhou, L., Li, M., Hu, Z.C., Guo, J.L., Yuan, H.L., Gong, H.J., Xiao, G.Q., Wei, J.Q., 2011. Age and growth of the Archean Kongling terrain, South China, with emphasis on 3.3 Ga granitoid gneisses. Am. J. Sci. 311, 153–182.
Greentree, M.R., Li, Z.X., Li, X.H., Wu, H.C., 2006. Late Mesoproterozoic to earliest Neoproterozoic basin record of the Sibao orogenesis in western South China and relationship to the assembly of Rodinia. Precamb. Res. 151, 79–100.
Guangdong BGMR (Bureau of Geology and Mineral Resources of Guangdong Province), 1988. Regional Geology of the Guangdong Province. Geological Publishing House, Beijing, pp. 1–941 (in Chinese with English abstract).
Harris, N.B.W., Inger, S., 1992. Trace element modelling of pelite-derived granites. Contrib. Mineral. Petrol. 110, 46–56.
Harris, N.B.W., Marzouki, F.M.H., Ali, S., 1986. The Jabel Sayid complex, Arabian shield: geochemical constraints on the origin of peralkaline and related granites. J. Geol. Soc. 143, 287–295.
Healy, B., Collins, W.J., Richards, S.W., 2004. A hybrid origin for Lachlan S-type granites: the Murrumbridgee batholith example. Lithos 79, 197–216.
Huang, X., Depaolo, D.J., 1989. Study of sources of Paleozoic granittoids and the basement of South China by means of Sr–Nd isotope. Acta Petrol. Sin. (1), 28–36.
Jayananda, M., Moyen, J.F., Martin, H., Peucat, J.J., Auvray, B., Mahabaleswar, B., 2000. Late Archaean (2550–2520 Ma) juvenile magmatism in the Eastern Dharwar craton, southern India: constraints from geochronology, Nd-Sr isotopes and whole rock geochemistry. Precamb. Res. 99, 225–254.
Jiao, W.F., Wu, Y.B., Yang, S.H., Peng, M., Wang, J., 2009. The oldest basement rock in the Yangtze craton revealed by zircon U–Pb age and Hf isotope composition. Sci. China: Earth Sci. 52, 1393–1399.
Kemp, A.I.S., Hawkesworth, C.J., Collins, W.J., Gray, C.M., Blevin, P.L., 2009. Isotopic evidence for rapid continental growth in an extensional accretionary orogen: the Tasmanides, eastern Australia. Earth Planet. Sci. Lett. 284, 455–466.
Li, W.X., Li, X.H., 2003. Adakitic granites within the NE Jiangxi ophiolite, South China: geochemical and Nd isotopic evidence. Precamb. Res. 122, 29–44.
Li, W.X., Li, X.H., Li, Z.X., 2005. Neoproterozoic bimodal magmatism in the Cathaysia Block of South China and its tectonic significance. Precamb. Res. 136 (1), 51–66.
Li, W.X., Li, X.H., Li, Z.X., 2010b. Ca. 850 Ma bimodal volcanic rocks in northeastern Jiangxi South China: initial extension during the breakup of Rodinia. Am. J. Sci. 310, 951–980.
Li, W.X., Li, X.H., Li, Z.X., Lou, F.S., 2008a. Obduction-type granites within the NE Jiangxi Ophiolite: implications for the final amalgamation between the Yangtze and Cathaysia Blocks. Gondwana Res. 13, 288–301.
Li, X.H., Li, W.X., Li, Z.X., Liu, Y., 2008b. 850–790 Ma bimodal volcanic and intrusive rocks in northern Zhejiang, South China: a major episode of continental rift magmatism during the breakup of Rodinia. Lithos 102 (1–2), 341–357.
Li, X.H., Li, W.X., Li, Z.X., Lo, C.H., Wang, J., Ye, M.F., Yang, Y.H., 2009. Amalgamation between the Yangtze and Cathaysia Blocks in South China: constraints from SHRIMP U–Pb zircon ages, geochemistry and Nd–Hf isotopes of the Shuangxiwu volcanic rocks. Precamb. Res. 174 (1–2), 117–128.
Li, Z.X., Bogdanova, S.V., Collins, A.S., Davidson, A., DeWaele, B., Ernst, R.E., Fitzsimons, I.C.W., Fuck, R.A., Gladkochub, D.P., Jacobs, J., Karlstrom, K.E., Lu, S., Natapov, L.M., Pease, V., Pisarevsky, S.A., Thrane, K., Vernikovsky, V., 2008c. Assembly, configuration, and breakup history of Rodinia: a synthesis. Precamb. Res. 160, 179–210.
Li, Z.X., Li, X.H., Wartho, J.A., Clark, C., Li, W.X., Zhang, C.L., Bao, C.M., 2010. Magmatic and metamorphic events during the Early Paleozoic Wuyi-Yunkai Orogeny, southeastern South China: new age constraints and P–T conditions. GSA Bull. 122 (5–6), 772–793.
Li, Z.X., Li, X.H., Zhou, H., Kinny, P.D., 2002. Grenvillian continental collision in South China: new SHRIMP U–Pb zircon results and implications for the configuration of Rodinia. Geology 30, 163–166.
Li, Z.X., Zhang, L., Powell, C.M., 1995. South China in Rodinia: part of the missing link between Australia-East Antarctica and Laurentia? Geology 23, 407–410.
Liang, X.R., Wei, G.J., Li, X.H., Liu, Y., 2003. Precise measurement of $^{143}Nd/^{144}Nd$ and Sm/Nd ratios using multiple-collectors inductively coupled plasma-mass spectrometer (MC-ICPMS). Geochimica 32, 91–96 (in Chinese with English abstract).
Liu, B.X., Liu, C.G., Qiu, Y.Q., 2001. The Pb–Pb isotopic ages and geologic significance of gneissic granite in Hezi, Jiangxi. Volcanol. Miner. Res. 22 (4), 264–268 (in Chinese with English abstract).

Liu, X.M., Gao, S., Diwu, C.R., Ling, W.L., 2008. Precambrian crustal growth of Yangtze craton as revealed by detrital zircon studies. Am. J. Sci. 308, 421–468.
Ludwig, K.R., 2001. Users manual for Isoplot/Ex rev. 2.49, A Geochronological Toolkit for Microsoft Excel. Berkeley Geochronology Center, Special Publication, Berkeley, California, No.1a, 55 pp.
Ma, T.Q., Chen, L.X., Bai, D.Y., Zhou, K.J., Li, G., Wang, X.H., 2009. Zircon SHRIMP dating and geochemical characteristics of Neoproterozoic granites of northeastern Hunan. Geol. China 36 (1), 65–73 (in Chinese with English abstract).
Patiño-Douce, A.E., Harris, N., 1998. Experimental constraints on Himalayan anatexis. J. Petrol. 39 (4), 689–710.
Pearce, J.A., 1996. Sources and settings of granitic rocks. Episodes 19, 120–125.
Pearce, J.A., Harris, N.B.W., Tindle, A.G., 1984. Trace element discrimination diagrams for the tectonic interpretation of granitic rocks. J. Petrol. 25, 956–983.
Qiu, Y.M., Gao, S., McNaughton, N.J., Groves, D.I., Ling, W.L., 2000. First evidence of >3.2 Ga continental crust in the Yangtze craton of South China and its implications for Archean crustal evolution and Phanerozoic tectonics. Geology 28 (1), 11–14.
Shu, L.S., Deng, P., Yu, J.H., Wang, Y.B., Jiang, S.Y., 2008. The age and tectonic environment of the rhyolitic rocks on the western side of Wuyi Mountain, South China. Sci China (Ser. D) 51 (8), 1053–1063.
Shu, L.S., Faure, M., Yu, J.H., Jahn, B.M., 2011. Geochronological and geochemical features of the Cathaysia block (South China): New evidence for the Neoproterozoic breakup of Rodinia. Precamb. Res. 187 (3–4), 263–276.
Shu, L.S., Faure, M., Jiang, S.Y., Yang, Q., Wang, Y.J., 2006. SHRIMP zircon U–Pb age, litho- and biostratigraphic analyses of the Huaiyu Domain in South China – evidence for a Neoproterozoic orogen, not Late Paleozoic-Early Mesozoic collision. Episodes 29, 244–252.
Sun, S.S., McDonough, W.F., 1989. Chemical and isotopic systematics of oceanic basalts: implication for mantle composition and process. In: Sauders, A.D., Norry, M.J. (Eds.), Magmatism in the Ocean Basins, vol. 42. Geol. Soc. Spec. Pub., pp. 313–345.
Sylvester, P.J., 1998. Postcollisional strongly peraluminous granites. Lithos 45, 29–44.
Taylor, S.R., McLennan, S.M., 1985. The Continental Crust: Its Composition and Evolution. Oxford Press Blackwel, Washington, DC, pp. 1–312.
Torsvik, T.H., Carter, L.M., Ashwal, L.D., Bhushan, S.K., Pandit, M.K., Jamtveit, B., 2001. Rodinia refined or obscured: palaeomagnetism of the Malani igneous suite (NW India). Precamb. Res. 108, 319–333.
Wan, Y.S., Liu, D.Y., Wilde, S.A., Cao, J.J., Chen, B., Dong, C.Y., Song, B., Du, L.L., 2010. Evolution of the Yunkai Terrane, South China: evidence from SHRIMP zircon U–Pb dating, geochemistry and Nd isotope. J. Asian Earth Sci. 37, 140–153.
Wan, Y.S., Liu, D.Y., Xu, M., Zhuang, J., Song, B., Shi, Y., Du, Y.L., 2007. SHRIMP U–Pb zircon geochronology and geochemistry of metavolcanic and metasedimentary rocks in Northwestern Fujian, Cathaysia block, China: Tectonic implications and the need to redefine lithostratigraphic units. Gondwana Res. 12 (1–2), 166–183.
Wang, J., Li, Z.X., 2003. History of Neoproterozoic rift basins in South China: implications for Rodinia breakup. Precamb. Res. 122 (1–4), 141–158.
Wang, L.J., Griffin, W.L., Yu, J.H., O'Reilly, S.Y., 2010a. Precambrian crustal evolution of the Yangtze Block tracked by detrital zircons from Neoproterozoic sedimentary rocks. Precamb. Res. 177 (1–2), 131–144.
Wang, L.J., Yu, J.H., O'Reilly, S.Y., Griffin, W.L., Wei, Z.Y., Jiang, S.Y., Sun, T., 2008a. Grenvillian orogeny in the Southern Cathaysia block: constraints from U–Pb ages and Lu–Hf isotopes in zircon from metamorphic basement. Chin. Sci. Bull. 53 (19), 3037–3050.
Wang, X.L., Zhou, J.C., Qiu, J.S., Zhang, W.L., Liu, X.M., Zhang, G.L., 2006. LA-ICP-MS U–Pb zircon geochronology of the Neoproterozoic igneous rocks from Northern Guangxi, South China, implications for petrogenesis and tectonic evolution. Precamb. Res. 145 (1–2), 111–130.
Wang, X.L., Shu, L.S., Xing, G.F., Zhou, J.C., Tang, M., Shu, X.J., Qi, L., Hu, Y.H., 2011a. Post-orogenic extension in the eastern part of the Jiangnan orogen: evidence from ca 800–760 Ma volcanic rocks. Precamb. Res., http://dx.doi.org/10.1016/j.precamres.2011.07.003.
Wang, X.L., Zhou, J.C., Griffin, W.L., Wang, R.C., Qiu, J.S., O'Reilly, S.Y., Xu, X.S., Liu, X.M., Zhang, G.L., 2007b. Detrital zircon geochronology of Precambrian basement sequences in the Jiangnan orogen: dating the assembly of the Yangtze and Cathaysia bocks. Precamb. Res. 159 (1–2), 117–131.
Wang, X.L., Zhou, J.C., Qiu, J.S., Jiang, S.Y., Shi, Y.R., 2008c. Geochronology and geochemistry of Neoproterozoic mafic rocks from western Hunan, South China: implications for petrogenesis and post-orogenic extension. Geol. Mag. 145 (2), 215–233.
Wang, Y.J., Fan, W.M., Sun, M., Liang, X.Q., Zhang, Y.H., Peng, T.P., 2007a. Geochronological, geochemical and geothermal constraints on petrogenesis of the Indosinian peraluminous granites in the South China Block: a case study in the Hunan Province. Lithos 96, 475–502.
Wang, Y.J., Fan, W.M., Zhang, G.W., Zhang, Y.H., 2013a. Phanerozoic tectonics of the South China Block: key observations and controversies. Gondwana Res. 23, 1273–1305.
Wang, Y.J., Fan, W.M., Zhao, G.C., Ji, S.C., Peng, T.P., 2007c. Zircon U–Pb geochronology of gneisses in Yunkai Mountains and its implications on the Caledonian event in South China. Gondwana Res. 12 (4), 404–416.
Wang, Y.J., Wu, C.M., Zhang, A.M., Fan, W.M., Zhang, Y.H., Zhang, Y.Z., Peng, T.P., Yin, C.Q., 2012c. Kwangsian and Indosinian reworking of the eastern South China Block: constraints on zircon U–Pb geochronology and metamorphism of amphibolite and granulite. Lithos 127, 239–260.
Wang, Y.J., Zhang, F.F., Fan, W.M., Zhang, G.W., Chen, S.Y., Cawood, P.A., Zhang, A.M., 2010b. Tectonic setting of the South China Block in the early Paleozoic: Resolving intracontinental and ocean closure models from detrital zircon U–Pb geochronology. Tectonics 29, http://dx.doi.org/10.1029/2010TC002750.
Wang, Y.J., Zhang, A.M., Cawood, P.A., Fan, W.M., Xu, J.F., Zhang, G.W., Zhang, Y.Z., 2013b. Geochronological, geochemical and Nd-Hf-Os isotopic fingerprinting of an early Neoproterozoic arc-back-arc system in South China and its accretionary assembly along the margin of Rodinia. Precamb. Res. 231, 343–371.
Wang, Y.J., Zhang, A.M., Fan, W.M., Zhao, G.C., Zhang, G.W., Zhang, Y.Z., Zhang, F.F., Li, S.Z., 2011b. Kwangsian crustal anatexis within the eastern South China Block: geochemical, zircon U–Pb geochronological and Hf isotopic fingerprints from the gneissoid granites of Wugong and Wuyi and Yunkai Domains. Lithos 127, 239–260.
Wei, G.J., Liang, X.R., Li, X.H., Liu, Y., 2002. Precise measurement of Sr isotopic composition of liquid and solid base using (LP) MC-ICPMS. Geochimica 31, 295–299.
Wu, R.X., Zheng, Y.F., Wu, Y.B., Zhao, Z.F., Zhang, S.B., Liu, X.M., Wu, F.Y., 2006. Reworking of juvenile crust, element and isotope evidence from Neoproterozoic granodiorite in South China. Precamb. Res. 146, 179–212.
Xia, X.P., Sun, M., Zhao, G.C., Li, H.M., Zhou, M.F., 2004. Spot zircon U–Pb isotope analysis by ICP-MS coupled with a frequency quintupled (213 nm) Nd-YAG laser system. Geochem. J. 38, 191–200.
Xu, X.S., O'Reilly, S.Y., Griffin, W.L., Deng, P., Pearson, N.J., 2005. Relict proterozoic basement in the Nanling Mountains (SE China) and its tectonothermal overprinting. Tectonics 24 (2), TC2003.
Yang, Z.Y., Sun, Z.M., Yang, T.S., Pei, J.L., 2004. A long connection (750–380 Ma) between South China and Australia: paleomagnetic constraints. Earth Planet. Sci. Lett. 220, 423–434.
Ye, M.F., Li, X.H., Li, W.X., Liu, Y., Li, Z.X., 2007. SHRIMP zircon U–Pb geochronological and whole-rock geochemical evidence for an early Neoproterozoic Sibaoian magmatic arc along the southeastern margin of the Yangtze Block. Gondwana Res. 12, 144–156.
Yu, J.H., O'Reilly, Y.S., Wang, L.J., Griffin, W.L., Jiang, S.Y., Wang, R.C., Xu, X.S., 2007. Finding of ancient materials in Cathaysia and implication for the formation of Precambrian crust, Chinese Science Bullet in Chin. Sci. Bull. 52, 13–22.
Yu, J.H., O'Reilly, Y.S., Wang, L.J., Griffin, W.L., Zhou, M.F., Zhang, M., Shu, L.S., 2010a. Components and episodic growth of Precambrian crust in the Cathaysia Block, South China: Evidence from U–Pb ages and Hf isotopes of zircons in Neoproterozoic sediments. Precamb. Res. 181, 97–114.
Yu, J.H., O'Reilly, Y.S., Zhou, M.F., Griffin, W.L., Wang, L.J., 2010b. U–Pb geochronology and Hf–Nd isotopic geochemistry of the Badu Complex, Southeastern China: Implications for the Precambrian crustal evolution and paleogeography of the Cathaysia Block. Precamb. Res. 222–223, 424–449.
Yu, J.H., Wang, L.J., Griffin, W.L., O'Reilly, S.Y., Zhang, M., Li, C.Z., Shu, L.S., 2009. A Paleoproterozoic orogeny recorded in a long-lived cratonic remnant (Wuyishan terrane), eastern Cathaysia Block, China. Precamb. Res. 174 (3–4), 347–363.
Yu, J.H., Zhou, X.M., O'Reilly, S.Y., 2005. Formation history and protolith characteristics of granulite facies metamorphic rock in Central Cathaysia deduced from U–Pb and Lu–Hf isotopic studies of single zircon grains. Chin. Sci. Bull. 50 (18), 2080–2089.
Zeng, W., Zhang, L., Zhou, H.W., Zhong, Z.Q., Xiang, H., Liu, R., Jin, S., Lu, X.Q., Li, C.Z., 2008. Caledonian reworking of Paleoproterozoic basement in the Cathaysia Block: constraints from zircon U–Pb dating, Hf isotopes and trace elements. Chin. Sci. Bull. 53 (6), 895–904.
Zhang, A.M., Wang, Y.J., Fan, W.M., Zhang, Y.Z., Yang, J., 2012a. Earliest Neoproterozoic (ca. 1.0 Ga) arc-back-arc-basin nature along the northern Yunkai Domain of the Cathaysia Block: geochronological and geochemical evidence from the metabasite. Precamb. Res. 220–221, 217–233.
Zhang, F.F., Wang, Y.J., Fan, W.M., Zhang, A.M., Zhang, Y.Z., 2011a. Zircon U–Pb geochronology and Hf isotopes of the Neoproterozoic granites in the Central Jiangxi Province. Geotecton. Metall. 35 (1), 73–84.
Zhang, Y.Z., Wang, Y.J., Fan, W.M., Zhang, A.M., Zhang, F.F., 2012b. Geochronological and geochemical constraints on the metasomatised source for the Neoproterozoic (~825 Ma) high-mg volcanic rocks from the Cangshuipu area (Hunan Province) along the Jiangnan Domain and their tectonic implications. Precamb. Res. 220–221, 139–157.
Zhang, Y.Z., Wang, Y.J., Geng, H.Y., Zhang, Y.H., Fan, W.M., Zhong, H., 2013. Early Neoproterozoic (~850 Ma) back-arc basin in the Central Jiangnan Orogen (Eastern South China): geochronological and petrogenetic constraints from meta-basalts. Precamb. Res. 231, 325–342.
Zhang, Z.L., Yuan, H.H., Nan, Y., 1997. Whole grain zircon evaporation for age of Luoyu Formation, Yunkai. Group. Minerl. Petrol. 18, 85–90 (in Chinese with English abstract).
Zhao, G.C., Cawood, P.A., 1999. Tectonothermal evolution of the Mayuan assemblage in the Cathaysia Block: new evidence for Neoproterozoic collisional-related assembly of the South China craton. Am. J. Sci. 299, 309–339.
Zhao, G.C., Cawood, P.A., 2012. Precambian geology of China. Precamb. Res. 222–223, 13–54.
Zhao, J.H., Zhou, M.F., Yan, D.P., Zheng, J.P., Li, J.W., 2011. Reappraisal of the ages of Neoproterozoic strata in South China: no connection with the Grenvillian orogeny. Geology 39, 299–302.
Zhao, J.H., Zhou, M.F., Zheng, J.P., 2013. Constraints from zircon U–Pb ages, O and Hf isotopic compositions on the origin of Neoproterozoic peraluminous

granitoids from the Jiangnan Fold Belt, South China. Contrib. Mineral. Petrol. 166, 1505–1519.

Zhejiang BGMR (Bureau of Geology and Mineral Resources of Zhejiang Province), 1989. Regional Geology of the Zhejiang Province. Geological Publishing House, Beijing, pp. 1–688 (in Chinese with English abstract).

Zheng, Y.F., Wu, R.X., Wu, Y.B., Zhang, S.B., Yuan, H.L., Wu, F.Y., 2008. Rift melting of juvenile arc-derived crust: geochemical evidence from Neoproterozoic volcanic and granitic rocks in the Jiangnan Orogen, South China. Precamb. Res. 163, 351–383.

Zheng, Y.F., Zhang, S.B., Zhao, Z.F., Wu, Y.B., Li, X.H., Li, Z.X., Wu, F.Y., 2007. Contrasting zircon Hf and O isotopes in the two episodes of Neoproterozoic granitoids in South China: implications for growth and reworking of continental crust. Lithos 96, 127–150.

Zhou, J.C., Wang, X.L., Qiu, J.S., 2009. Geochronology of Neoproterozoic mafic rocks and sandstones from northeastern Guizhou, South China: coeval arc magmatism and sedimentation. Precamb. Res. 170, 27–42.